The Astrophysical Journal, 653:1004–1026, 2006 December 20

A SPECTROSCOPIC SURVEY OF REDSHIFT $1.4 \lesssim z \lesssim 3.0$ GALAXIES IN THE GOODS-NORTH FIELD: SURVEY DESCRIPTION, CATALOGS, AND PROPERTIES[1]

Naveen A. Reddy,[2,3] Charles C. Steidel,[2] Dawn K. Erb,[4] Alice E. Shapley,[5] and Max Pettini[6]

Received 2006 May 7; accepted 2006 September 1

ABSTRACT

We present the results of a spectroscopic survey with LRIS-B on Keck of more than 280 star-forming galaxies and AGNs at redshifts $1.4 \lesssim z \lesssim 3.0$ in the GOODS-N field. Candidates are selected by their $U_nG\mathcal{R}$ colors using the "BM/BX" criteria to target redshift $1.4 \lesssim z \lesssim 2.5$ galaxies and the LBG criteria to target redshift $z \sim 3$ galaxies; combined these samples account for ~25%–30% of the $\mathcal{R}$ and K_s band counts to $\mathcal{R} = 25.5$ and $K_s(\mathrm{AB}) = 24.4$, respectively. The 212 BM/BX galaxies and 74 LBGs constitute the largest spectroscopic sample of galaxies at $z > 1.4$ in GOODS-N. Extensive multiwavelength data allow us to investigate the stellar populations, stellar masses, bolometric luminosities (L_{bol}), and extinction of $z \sim 2$ galaxies. Deep *Chandra* and *Spitzer* data indicate that the sample includes galaxies with a wide range in L_{bol} ($\simeq 10^{10}$ to $>10^{12}\ L_{\odot}$) and 4 orders of magnitude in dust obscuration ($L_{\mathrm{bol}}/L_{\mathrm{UV}}$). The sample includes galaxies with a large dynamic range in evolutionary state, from very young galaxies (ages ≃50 Myr) with small stellar masses ($M^* \simeq 10^9\ M_{\odot}$) to evolved galaxies with stellar masses comparable to the most massive galaxies at these redshifts ($M^* > 10^{11}\ M_{\odot}$). *Spitzer* data indicate that the optical sample includes some fraction of the obscured AGN population at high redshifts: at least 3 of 11 AGNs in the $z > 1.4$ sample are undetected in the deep X-ray data but exhibit power-law SEDs longward of ~2 μm (rest frame) indicative of obscured AGNs. The results of our survey indicate that rest-frame UV selection and spectroscopy presently constitute the most timewise *efficient* method of culling large samples of high-redshift galaxies with a wide range in intrinsic properties, and the data presented here will add significantly to the multiwavelength legacy of GOODS.

Subject headings: cosmology: observations — galaxies: active — galaxies: evolution — galaxies: high-redshift — galaxies: starburst — galaxies: stellar content

Online material: color figure

1. INTRODUCTION

Rapid advances in our understanding of galaxy evolution have been prompted by the recognition that observations covering the full spectrum are necessary to adequately interpret the physical nature of galaxies. Multicolor *Hubble Space Telescope* (*HST*) imaging of two otherwise inconspicuous fields in the high Galactic latitude sky (Williams et al. 1996, 2000) marked the inception of a decade dominated by large-scale multiwavelength surveys. The two Hubble Deep Fields are now encompassed or supplanted by other areas of the sky that are the focus of a number of space- and ground-based observations both within and peripheral to the Great Observatories Origins Deep Survey (GOODS; Dickinson et al. 2003b). Included among these data are the deepest *Chandra* X-ray observations (Alexander et al. 2003), *HST* Advanced Camera for Surveys (ACS) optical imaging (Giavalisco et al. 2004), *Spitzer* IR to far-IR imaging (M. Dickinson et al. 2006, in preparation; R. Chary et al. 2006, in preparation), *GALEX* far- and near-UV imaging (Schiminovich et al. 2003), ground-based optical and near-IR imaging and spectroscopy (Capak et al. 2004; Cowie et al. 2004; Vanzella et al. 2005), and radio/submillimeter observations (Richards 2000; Pope et al. 2005).

Despite the easy access to broadband photometry and subsequent insights into galaxy evolution made possible by multiwavelength surveys such as GOODS, important issues regarding survey completeness and the physical conditions in galaxies and their surrounding intergalactic medium (IGM) can only be investigated spectroscopically. Spectroscopy of galaxies in blind flux-limited surveys can be quite inefficient and expensive, particularly if one only wants to study galaxies at certain cosmological epochs. However, we have shown that the technique of photometric preselection can allow one to cull large samples of galaxies in particular redshift ranges over a large range in redshift $1.0 \lesssim z \lesssim 4$ (e.g., Adelberger et al. 2004; Steidel et al. 1995, 2003, 2004; Steidel & Hamilton 1993), which can then be efficiently followed up using multiobject optical spectrographs such as the Low Resolution Imaging Spectrograph (LRIS) on the 10 m Keck telescope. Near-UV sensitive spectrographs such as the blue arm of LRIS (LRIS-B) on Keck and the Focal Reducer/low-dispersion Spectrograph (FORS) on the VLT have significantly extended our capabilities by allowing for spectroscopy of key features that fall shortward of the OH emission forest for redshifts $1.4 \lesssim z \lesssim 3$, a particularly active epoch in the context of galaxy evolution and the buildup of stellar and black hole mass. To take advantage of extensive multiwavelength data, we included the GOODS-North (hereafter GOODS-N) field in our ongoing survey to select and spectroscopically follow up large samples of galaxies at redshifts $1.4 \lesssim z \lesssim 3.0$ (Steidel et al. 2004). In the interest of public dissemination of data, we present in this paper the results of our spectroscopic survey of $1.4 \lesssim z \lesssim 3.0$ star-forming galaxies in the GOODS-N field including associated photometry and spectroscopic redshifts. Information on the galaxies, including their photometric

[1] Based on data obtained at the W. M. Keck Observatory, which is operated as a scientific partnership among the California Institute of Technology, the University of California, and NASA and was made possible by the generous financial support of the W. M. Keck Foundation.

[2] California Institute of Technology, MS 105-24, Pasadena, CA 91125.

[3] National Optical Astronomy Observatory, 950 North Cherry Avenue, Tucson, AZ 85719.

[4] Harvard-Smithsonian Center for Astrophysics, 60 Garden Street, Cambridge, MA 02138.

[5] Department of Astrophysical Sciences, Peyton Hall, Ivy Lane, Princeton, NJ 08544.

[6] Institute of Astronomy, Madingley Road, Cambridge CB3 OHA, UK.

measurements and errors and stellar population fits, are available online.[7]

The outline of this paper is as follows. In § 2 we briefly describe the optical imaging, photometry, and spectroscopy. To supplement these, we have also obtained the deepest wide-area near-IR *J*- and *K*-band imaging in the GOODS-N field, and these data are also presented in § 2. The spectroscopic results and associated catalog are presented in § 3. We describe the *Spitzer* IRAC and MIPS data (taken from the GOODS-N public release; M. Dickinson et al. 2006, in preparation; R. Chary et al. 2006, in preparation) for our spectroscopic sample of galaxies in § 4. Ground-based photometry and *Spitzer* IRAC data, together with spectroscopic redshifts, enable the modeling of the stellar populations of galaxies given certain simplifying assumptions. Our modeling procedure and results are discussed in § 5. In § 6 we describe a few characteristics of the sample of star-forming galaxies and active galactic nuclei (AGNs) to demonstrate the wide range in intrinsic properties of UV-selected galaxies at high redshift. A flat ΛCDM cosmology is assumed with $H_0 = 70$ km s^{-1} Mpc^{-1} and $\Omega_\Lambda = 0.7$. All magnitudes are on the AB (Oke & Gunn 1983) system.

2. DATA AND SAMPLE SELECTION

2.1. *Optical and Near-IR Imaging and Photometry*

The imaging, photometry, color selection, and spectroscopic observations of galaxies in the fields of our $z \sim 2$ survey are described in several other papers published by our group (Steidel et al. 2003, 2004; Adelberger et al. 2004; Reddy et al. 2005). Specific details regarding the GOODS-N optical imaging are presented in Reddy et al. (2005) and summarized below for convenience.

The optical images used to photometrically preselect candidate galaxies at redshifts $1.4 \lesssim z \lesssim 3.0$ in the GOODS-N field were obtained in 2002 and 2003 April with the Kitt Peak National Observatory (KPNO) and Keck I telescopes. The KPNO MOSAIC *U*-band image obtained from the GOODS team (PI: Giavalisco) was transformed to U_n magnitudes (Steidel et al. 2004). The Keck I *G*- and $\mathcal{R}$-band images were taken with the LRIS instrument (Oke et al. 1995; Steidel et al. 2004) and were oriented to ensure maximum overlap with the GOODS *Spitzer* Legacy and *Hubble* Treasury programs. The images cover $11' \times 15'$ with FWHM $\sim 0\farcs7$–$1\farcs1$ to a limiting magnitude of ~27.5 measured within a $1''$ aperture (3 σ) in the $U_nG\mathcal{R}$ bands. This depth ensures that we are complete to $\mathcal{R} = 25.5$, neglecting photometric scatter, for galaxies whose colors satisfy our $z \sim 2$–3 color criteria. The optical imaging reduction and photometry were done following the procedures described in Steidel et al. (2003, 2004). The images were astrometrically calibrated using the SDSS database. Source detection is done at $\mathcal{R}$ band, and $G - \mathcal{R}$ and $U_n - G$ colors are computed by applying the $\mathcal{R}$-band isophotal apertures to images in the other filters.

We have obtained very deep wide-area near-IR imaging at *J* and K_s band in the GOODS-N field from observations with the Wide Field Infrared Camera (WIRC; Wilson et al. 2003) on the Palomar Hale 5 m telescope. The images, taken under photometric conditions with ~1.″0 FWHM, reach a depth of $K_s \sim 24.4$ and $J \sim 25.0$ over the central $8\farcm7 \times 8\farcm7$ of the GOODS-N field. The near-IR imaging reduction procedure is described in detail by Erb et al. (2006c). Near-IR magnitudes were calibrated in Vega magnitudes and converted to AB units assuming the following conversions: $K_s(\mathrm{AB}) = K_s(\mathrm{Vega}) + 1.82$ and $J(\mathrm{AB}) = J(\mathrm{Vega}) + 0.90$. Figure 1 shows the area imaged in the near-IR with respect to our optical image of the GOODS-N field.

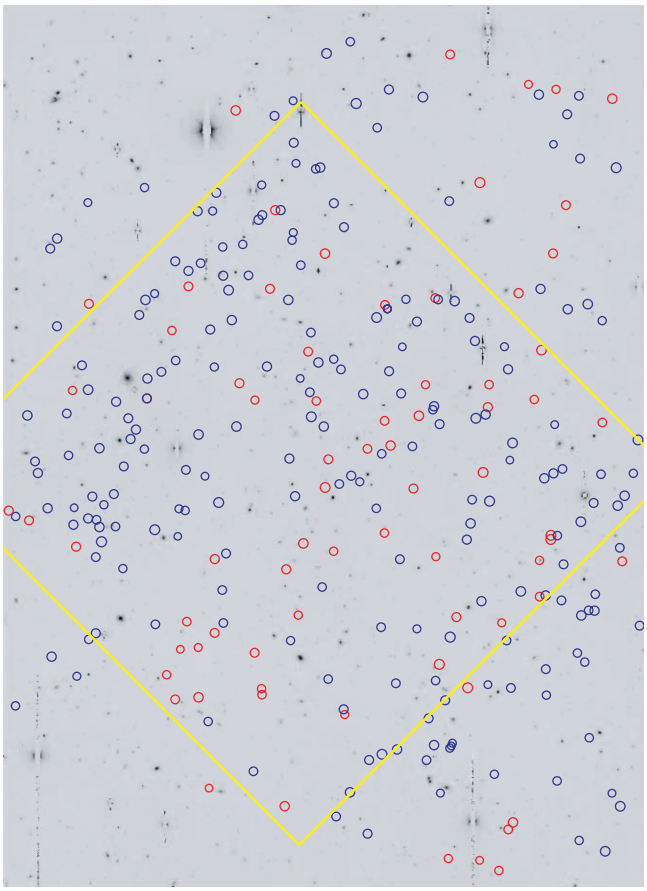

FIG. 1.—Positions of BX/BM (*blue circles*) and LBG (*red circles*) galaxies with spectroscopic redshifts $z > 1.4$ overlaid on our $10' \times 15'$ optical $\mathcal{R}$-band image of the GOODS-N field. The yellow box ($8\farcm5 \times 8\farcm5$) indicates the region with deep *J* and K_s Palomar imaging.

Photometric errors for both optical and near-IR magnitudes were determined from Monte Carlo simulations. We added large numbers of simulated galaxies with known magnitudes to our images and then recovered them using the same photometric method used to detect actual galaxies. Comparing the input magnitudes with those recovered then yields an estimate of the bias and uncertainty in our photometry. The Monte Carlo method is discussed in more detail by Shapley et al. (2005). The typical errors in the optical and near-IR magnitudes range from 0.05 to 0.3 mag.

2.2. *Photometric Selection*

We selected galaxies in different redshift ranges between $1.4 \lesssim z \lesssim 3.4$ using the "BM," "BX," "C," "D," and "MD" selection criteria (Steidel et al. 2003, 2004; Adelberger et al. 2004). The C, D, and MD criteria are used to select Lyman break galaxies (LBGs) at redshifts $2.7 \lesssim z \lesssim 3.3$ (Steidel et al. 2003).[8] The BM and BX criteria were designed to cull galaxies at redshifts $1.4 \lesssim z \lesssim 2.0$ and $2.0 \lesssim z \lesssim 2.5$, respectively, with approximately the same range of UV luminosity and intrinsic UV color as the $z \sim 3$ LBGs (Adelberger et al. 2004; Steidel et al.

[7] See http://www.astro.caltech.edu/~drlaw/GOODS/.

[8] Note that we did not select M galaxies in GOODS-N as was done in other fields of the $z \sim 3$ survey (Steidel et al. 2003).

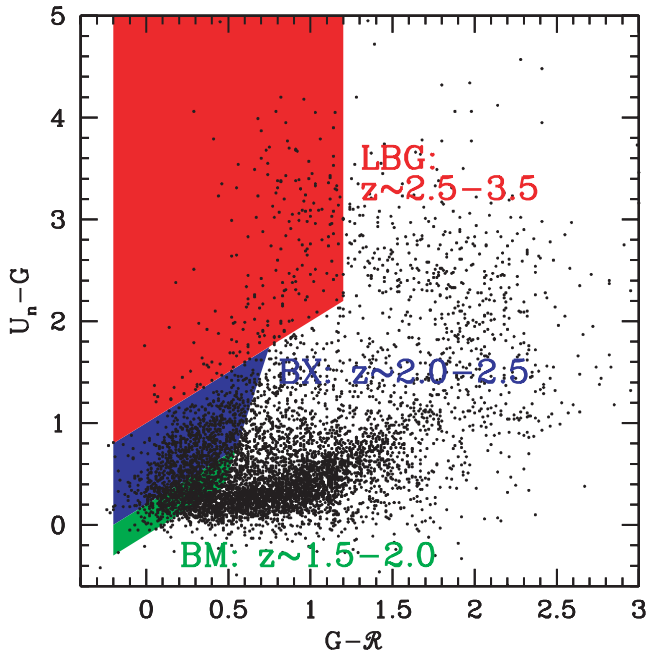

FIG. 2.—$U_nG\mathcal{R}$ colors of objects with $\mathcal{R} < 25.5$ in the GOODS-N field. Also shown are the LBG, BX, and BM selection windows.

2004). The various selection criteria considered here are shown in Figure 2. We only considered candidates to $\mathcal{R} = 25.5$ to ensure a sample of galaxies that are bright enough such that optical spectroscopy is feasible.[9] This limit corresponds to an absolute magnitude 0.6 mag fainter at $z \sim 2.2$ than at $z \sim 3$, based on the distance modulus between the two redshifts. We also excluded from the sample those candidates with $\mathcal{R} < 19$ since almost all of these objects are stars. Optical selection yielded 1360 BM/BX and 192 C/D/MD candidates in the $11' \times 15'$ area of the GOODS-N field. Combined, the BX/BM and C/D/MD candidates constitute ~30% of the $\mathcal{R}$-band counts to $\mathcal{R} = 25.5$. The number of candidates and their surface densities are listed in Table 1. Approximately 50% of these candidates lie in the region imaged at J and K_s. The remainder of this paper focuses on those galaxies that have been spectroscopically confirmed to lie at redshifts $z > 1.4$, as described in the next section.

[9] A few objects were candidates based on photometry of our Palomar images of the GOODS-N field (Steidel et al. 2003) but failed to satisfy the photometric selection criteria based on the newer Keck images. These objects are indicated in subsequent tables by their notation as presented in Steidel et al. (2003) or, in the case of BM/BX objects, by the letters "BX" or "BM" followed by no more than three numerical digits. The photometric values for these objects are the ones based on the new photometry.

2.3. *Optical Spectroscopy*

We took advantage of the multiobject capabilities of the Keck LRIS instrument to obtain spectroscopy for the photometrically selected candidates. In its upgraded double-armed capacity, LRIS makes use of a dichroic to send light to both a red and blue arm. The commissioning of the blue arm of LRIS (LRIS-B) allowed, for the first time, the ability to obtain very sensitive near-UV spectroscopic observations at wavelengths as short as ~3100 Å, essentially to the atmospheric transmission limit. The wavelength range from the atmospheric cutoff up to ~5500 Å is particularly useful for probing the rich set of interstellar and stellar lines between Lyα and C IV ($\lambda\lambda$1548, 1550) for galaxies in the so-called spectroscopic desert, between redshifts $1.4 \lesssim z \lesssim 2.5$. As shown previously in Adelberger et al. (2004) and Steidel et al. (2004), combining photometric selection of BM and BX candidates with the near-UV sensitivity of LRIS-B allows for the wholesale spectroscopy of large numbers of galaxies in this redshift range; this in turn enables us to focus our study on an epoch that was particularly active in terms of star formation and accretion activity (e.g., Dickinson et al. 2003a; Chapman et al. 2003; Fan et al. 2001; Madau et al. 1996; Shaver et al. 1996; Schmidt et al. 1995).

The instrumental setup used for spectroscopy in the GOODS-N field varied during the course of the $z \sim 2$ survey; the various setups are described in more detail by Steidel et al. (2004). We selected dichroic filters designed to split the incoming beam at 5600 Å or 6800 Å. To provide maximum throughput between 3100 and 4000 Å, we used a 400 groove mm^{-1} grism blazed at 3400 Å on LRIS-B, resulting in a dispersion of 1.09 Å pixel^{-1}. For simultaneous observations on the red side of LRIS (LRIS-R), we used a 400 groove mm^{-1} grating blazed at 8500 Å, providing wavelength coverage up to 9500 Å. We typically obtained simultaneous blue- and red-side spectroscopic observations between 3100 and 9500 Å, with slight variations due to the relative placement of slits in the telescope focal plane.

TABLE 1
SAMPLE STATISTICS TO $\mathcal{R} = 25.5$

Candidates	$N_{\rm cand}$[a]	$\rho_{\rm cand}$[b] (arcmin^{-2})	$N_{\rm obs}$[c]	$N_{z>1}$[d]	$f_{z>1}$[e]	$N_{z>1.4}$[f]	$\langle z \rangle$[g]
BM	470	3.13 ± 0.14	67	63	0.94	49	1.72 ± 0.34
BX	890	5.93 ± 0.20	205	170	0.83	163	2.19 ± 0.40
C	55	0.37 ± 0.05	26	26	0.97	26	3.11 ± 0.21
D	59	0.39 ± 0.05	23	23	0.98	23	3.05 ± 0.22
MD	78	0.52 ± 0.06	26	25	0.96	25	2.96 ± 0.30
Total	1552	10.35 ± 0.26	347	307	0.88	286	2.25 ± 0.57

[a] Number of photometric candidates.
[b] Surface density of photometric candidates to $\mathcal{R} = 25.5$.
[c] Number of objects with secure spectroscopic identifications.
[d] Number of objects with secure redshifts $z > 1$.
[e] Fraction of spectroscopically observed objects with $z > 1$. The foreground ($z < 1$) contamination rates of the C, D, and MD samples are very low (<5%), and we assume the interloper fractions derived over all fields of the $z \sim 3$ LBG survey (Steidel et al. 2003). For the BM and BX samples, we assume foreground contamination fractions derived from the GOODS-N field, which are similar to those derived in other fields of the $z \sim 2$ survey (Steidel et al. 2004).
[f] Number of objects with $z > 1.4$.
[g] Mean and standard deviation of redshift distribution for objects with $z > 1$.

The slit masks used for spectroscopy cover $8' \times 5'$ on the sky. For a minimum slit length of $9''$ (adopted in order to ensure good background subtraction), we are able to include 30–35 slits, in addition to four to five star boxes used to accurately align each mask. We set the width of each slit to $1''.2$, and this, combined with a typical seeing of $0''.8$, yields a typical resolution of 5 Å for point sources. To obtain the optimum mix of objects on any given slit mask, we assigned each candidate a weight primarily based on its optical magnitude. We gave larger weights to objects with $\mathcal{R} = 23.5$–24.5 and lower weights for fainter objects where absorption-line spectroscopy is more difficult and brighter objects where the foreground ($z \lesssim 1.0$) interloper fraction is larger. Nonetheless, we filled "blank" areas of the masks with filler objects that included these fainter and brighter objects. In particular, we included some bright ($\mathcal{R} < 23.5$) objects on masks since at least some of these are intrinsically bright $z \sim 2$–3 galaxies and are most suitable for detailed follow-up spectroscopic studies. To support other projects being conducted by our group, we also deliberately targeted objects within the $U_nG\mathcal{R}$ sample that had interesting multiwavelength properties, such as those identified with 850 μm or 24 μm emission, as well as those with unusually red near-IR colors. We also designed masks to overlap as much as possible with the near-IR imaging. Because of this, $\sim$73% of spectroscopically confirmed galaxies with $z > 1.4$ lie in the K_s band region, even though $\sim$50% of $U_nG\mathcal{R}$ candidates lie in the same region (see Fig. 1).

We typically obtained three exposures of 1800 s per mask, for a total exposure of 5400 s. The range in optical magnitudes implies a large range in the signal-to-noise ratio of the spectra. At the minimum, however, we found 5400 s to be sufficient to obtain redshifts, and a few objects were observed on more than one mask. The spectroscopic success rate per mask is primarily a function of the weather conditions (e.g., cirrus, seeing) at the time of observation, with a 90% success rate of obtaining redshifts in the best conditions; these redshifts, for the most part, fell within the targeted redshift ranges. This suggests that the redshift distributions for the spectroscopic and photometric samples are similar, and there are not large numbers of galaxies whose true redshifts are far from those expected based on their observed $U_nG\mathcal{R}$ colors. Details of the spectral reduction techniques are described in Steidel et al. (2003). We identified redshifts based on the presence of a number of low-ionization interstellar absorption lines (e.g., Si II λ1260, O I+S II λ1303, C II λ1334, Si II λ1526, Fe II λ1608, Al II λ1670, and Al III $\lambda\lambda$1854, 1862), stellar wind features (e.g., N V $\lambda\lambda$1238, 1242, S IV $\lambda\lambda$1393, 1402, and C IV $\lambda\lambda$1548, 1550), the C III λ1909 nebular emission line, or Lyα emission or absorption. A few examples of spectra are shown in Steidel et al. (2003, 2004). Spectroscopically confirmed galaxies with $1.4 < z < 3.0$ are shown with respect to the $\mathcal{R}$-band image of the GOODS-N field in Figure 1.

Comparison with nebular redshifts derived from Hα spectroscopy indicates that Lyα emission is almost always redshifted, and interstellar absorption lines are almost always blueshifted, with respect to the systemic (nebular) redshift of the galaxy. These systematic offsets have been interpreted as the result of outflows (e.g., Adelberger et al. 2003, 2005b; Pettini et al. 2001; Shapley et al. 2003). Adelberger et al. (2005b) present linear least-squares fits to the systemic redshifts of galaxies given their Lyα and interstellar absorption redshifts based on a sample of 138 objects with near-IR spectroscopy (Erb et al. 2006c; Pettini et al. 2001).

3. SPECTROSCOPIC RESULTS AND CATALOG

Our spectroscopic sample in the GOODS-N field presently includes 212 BM/BX and 74 C/D/MD galaxies with secure spectroscopic redshifts $z > 1.4$ (Table 2). The total sample includes 347 objects with secure spectroscopic redshifts, including 40 interlopers with $z < 1$. We also include 41 objects with uncertain redshifts in Table 2, denoted by a colon in the redshift field (for consistency with Steidel et al. 2003), for a total of 388 objects. Table 1 lists the statistics for the individual samples, including the numbers of candidates observed, the interloper fractions, and mean redshifts. The primary source of contamination in the LBG sample is from K dwarfs in the Galactic halo. Star-forming galaxies at redshift $\langle z \rangle = 0.17 \pm 0.09$ contaminate the BX sample since their Balmer breaks mimic the Lyα forest decrement. These interlopers can be easily excluded using K_s band photometry (e.g., the *BzK* criteria; Daddi et al. 2004), but we have not imposed any additional criteria other than the observed optical magnitudes and colors. The main "contaminants" of the BM sample occur from galaxies with redshifts $1.0 < z < 1.4$; these galaxies have $U_nG\mathcal{R}$ colors very similar to those of BM objects, and the narrow BM color selection window implies that photometric scatter and Lyα perturbations on the $U_nG\mathcal{R}$ colors can have a significant impact on the observed redshift distribution of BM galaxies (N. A. Reddy et al. 2006, in preparation). Throughout this paper we consider objects with $z < 1.4$ to be contaminants. The AGNs/QSOs (as identified from either their X-ray, UV, or *Spitzer* IRAC or MIPS emission) with $z > 1.4$ make up $\sim$4% of the sample (see § 6.2 for further discussion).

For consistency, we compared redshifts for objects in common with the Team Keck Treasury Redshift Survey (TKRS; Wirth et al. 2004; Cowie et al. 2004). We note that the TKRS is based primarily on observations with the DEIMOS instrument on Keck II, and so the TKRS redshift selection function rapidly declines above $z \sim 1.2$ as the emission and absorption lines used for redshift identification (including [N II], [S II], [O III], and [O II] emission features and calcium H and K absorption features) are shifted out of the DEIMOS spectral range. The overlap between the $U_nG\mathcal{R}$ and TKRS samples is small given that the two surveys target different redshifts (TKRS is better at identifying galaxies at $z \lesssim 1.2$, and our $U_nG\mathcal{R}$ selection is better at identifying galaxies at $z \gtrsim 1.4$).

There are 64 objects with redshifts in the $U_nG\mathcal{R}$ catalog that are also in the TKRS database. Of these, 52 were previously published in other surveys of the GOODS field (Cowie et al. 2004; Cohen et al. 1996, 2000; Cohen 2001; Barger et al. 2000, 2003; Wirth et al. 2004; Phillips et al. 1997; Lowenthal et al. 1997; Dawson et al. 2001; Steidel et al. 1996, 2003; Dickinson 1998) and/or have agreement in redshift between the $U_nG\mathcal{R}$ and TKRS samples. On further inspection of the 12 objects with discrepant redshifts, we adopted the TKRS redshift for six of them (BX1202, BX1371, BMZ1010, BMZ1100, BMZ1121, and BMZ1208); the redshifts for these six galaxies are all below $z < 1.4$, where the DEIMOS determination was found to be secure and where our BM selection function drops off. Five of the objects had the correct redshifts in our catalog (BX1299, BX1319, BX1805, BMZ1119, and BMZ1375). For the remaining object, BX1214, we were able to rule out the Cohen et al. (2000) redshift of $z = 2.500$ but were unable to confidently assign a redshift based on our LRIS spectrum.

The redshift distributions of BM/BX and LBG galaxies with $z_{\rm spec} > 1$ are shown in Figure 3, where the right panel emphasizes large-scale structure in the GOODS-N field. The redshift overdensity at $z = 2.95$ is prominent and was also noted in the LBG survey (Steidel et al. 2003). We also note a possible overdensity at $z = 2.00$, which corresponds to an overdensity of five submillimeter galaxies as noted by Blain et al. (2004). However, we caution that Figure 3 only presents raw numbers, and we have

TABLE 2

GOODS-N $U_nG\mathcal{R}$ Galaxies with Spectroscopic Redshifts

Name	α (J2000.0)	δ (J2000.0)	z_{em}[a]	z_{abs}[b]	Type[c]	$\mathcal{R}$[d] (mag)	$G-\mathcal{R}$ (mag)	U_n-G[e] (mag)	J[f] (mag)	K_s[f] (mag)	$m_{3.6\,\mu m}$ (mag)	$m_{4.5\,\mu m}$ (mag)	$m_{5.8\,\mu m}$ (mag)	$m_{8.0\,\mu m}$ (mag)	$f_{24\,\mu m}$ (μJy)	Notes[g]
BX1035	12 36 13.03	62 10 21.1	...	2.236	GAL	23.46	0.37	0.68	...	...	22.48 ± 0.09	22.47 ± 0.13	22.11 ± 0.14	22.59 ± 0.28	33.0 ± 6.3	
BX1040	12 36 17.81	62 10 11.2	2.469	2.466	GAL	24.84	0.22	0.68	...	...	22.94 ± 0.12	23.27 ± 0.21	...	...	...	
BX1042	12 35 50.89	62 13 33.5	2.613	2.601	GAL	24.83	0.50	1.16	...	...	23.09 ± 0.07	23.03 ± 0.10	23.13 ± 0.19	22.88 ± 0.18	15.2 ± 4.3	
BX1050	12 36 18.80	62 10 37.4	...	2.322	GAL	24.71	0.40	0.73	...	...	23.49 ± 0.09	23.51 ± 0.08	23.46 ± 0.30	...	...	
BX1051	12 35 52.97	62 13 36.8	...	2.098	GAL	24.23	0.14	0.57	...	...	23.07 ± 0.19	...	...	...	203.9 ± 14.4	
BX1055	12 35 59.59	62 13 07.5	2.496	2.486	GAL	24.09	0.24	0.81	...	...	23.12 ± 0.10	23.23 ± 0.14	...	...	...	
BX1060	12 36 06.40	62 12 29.1	...	2.081	GAL	24.22	0.43	0.84	...	...	21.74 ± 0.07	21.73 ± 0.08	21.93 ± 0.19	...	67.3 ± 8.3	
BX1064	12 36 30.34	62 09 45.3	...	2.086	GAL	24.20	0.28	0.61	23.60	22.63	23.00 ± 0.07	23.11 ± 0.08	23.16 ± 0.17	23.76 ± 0.32	26.0 ± 5.5	
BX1065	12 36 09.84	62 11 39.0	...	2.701	GAL	24.01	0.43	1.04	...	...	22.41 ± 0.07	22.60 ± 0.15	...	...	13.3 ± 3.9	
BX1069	12 36 45.82	62 08 08.2	0.000	0.000	STAR	21.95	0.38	0.77	...	...	23.37 ± 0.08	24.01 ± 0.16	...	...	...	
BX1071	12 36 20.10	62 11 12.6	...	1.996	GAL	24.41	0.27	0.76	23.71	24.10	22.84 ± 0.10	23.06 ± 0.21	...	...	...	
BX1073	12 36 43.35	62 08 19.6	0.087	0.087	GAL	20.59	0.40	0.82	...	...	21.71 ± 0.07	22.15 ± 0.07	22.66 ± 0.10	22.56 ± 0.24	41.2 ± 6.7	
BX1074	12 36 19.38	62 11 25.5	1.754	1.745	GAL	24.01	0.13	0.40	22.74	21.92	22.11 ± 0.07	22.09 ± 0.07	22.00 ± 0.23	...	40.5 ± 6.5	
BX1075	12 36 14.45	62 11 52.1	...	2.221	GAL	24.08	0.35	1.04	...	...	22.47 ± 0.11	22.49 ± 0.15	22.30 ± 0.22	...	10.8 ± 3.5	
BX1080	12 36 18.39	62 11 39.2	...	2.390	GAL	24.38	0.51	1.15	...	...	22.55 ± 0.07	22.53 ± 0.07	22.72 ± 0.23	23.02 ± 0.35	47.3 ± 7.0	S03-D7
BX1081	12 36 15.19	62 12 07.6	...	1.801	GAL	24.23	0.23	0.60	...	...	22.25 ± 0.07	22.33 ± 0.07	22.66 ± 0.24	22.79 ± 0.20	48.3 ± 7.1	
BX1084	12 36 13.57	62 12 21.5	...	2.437	GAL	23.24	0.26	0.72	...	...	22.29 ± 0.07	22.33 ± 0.07	22.19 ± 0.15	22.63 ± 0.18	54.3 ± 7.5	
BX1085	12 36 13.33	62 12 16.3	...	2.236	GAL	24.50	0.33	0.87	...	...	23.38 ± 0.09	23.52 ± 0.15	23.47 ± 0.32	...	...	
BX1086	12 36 13.42	62 12 18.8	2.444	2.444	GAL	24.64	0.41	1.09	...	...	23.25 ± 0.12	23.24 ± 0.13	...	...	...	z from Hα
BX1089	12 36 00.64	62 13 59.4	...	2.049	GAL	24.23	0.16	0.83	...	...	21.92 ± 0.07	21.95 ± 0.07	21.94 ± 0.17	21.83 ± 0.26	76.7 ± 9.2	
BX1100	12 36 39.65	62 09 48.4	...	2.079	GAL	23.20	0.17	0.61	22.85	22.11	22.22 ± 0.11	22.26 ± 0.16	22.19 ± 0.26	...	84.4 ± 9.3	
BX1104	12 36 18.35	62 12 22.2	2.445	2.438	GAL	24.03	0.18	0.78	...	...	23.03 ± 0.07	23.08 ± 0.07	23.26 ± 0.30	23.12 ± 0.28	24.5 ± 5.2	
BX1106	12 36 27.56	62 11 29.8	...	2.917	GAL	24.61	0.65	1.52	>25.0	24.05	23.07 ± 0.11	23.16 ± 0.21	22.88 ± 0.26	22.93 ± 0.32	8.5 ± 1.3	S03-oMD28
BX1112	12 36 15.65	62 13 05.3	0.170	...	GAL	24.26	0.21	0.87	...	...	24.18 ± 0.09	24.77 ± 0.21	...	...	...	
BX1116	12 36 09.05	62 13 59.1	...	2.048	GAL	24.10	0.13	0.62	...	...	22.59 ± 0.07	22.66 ± 0.07	22.50 ± 0.15	23.06 ± 0.14	18.4 ± 5.1	
BX1120	12 36 07.62	62 14 16.6	0.169	...	GAL	24.64	0.43	1.31	...	...	24.95 ± 0.21	...	...	...	...	
BX1121	12 36 13.24	62 13 39.6	1.878	1.878	GAL	23.80	0.13	0.46	...	...	21.77 ± 0.07	21.78 ± 0.07	22.07 ± 0.14	22.22 ± 0.14	55.5 ± 7.8	
BX1125	12 36 25.00	62 12 23.6	2.222	...	GAL	25.20	0.18	0.94	>25.0	>24.4	24.00 ± 0.14	24.37 ± 0.24	...	...	...	
BX1126	12 36 11.91	62 13 58.7	...	:1.942	GAL	24.59	0.07	0.32	...	...	23.61 ± 0.16	23.74 ± 0.25	...	...	...	
BX1129	12 36 56.94	62 08 48.7	...	1.973	GAL	22.80	0.21	0.58	...	...	21.52 ± 0.07	21.60 ± 0.07	21.46 ± 0.09	22.00 ± 0.13	104.4 ± 10.3	
BX1130	12 36 33.17	62 11 34.1	0.080	...	GAL	20.65	0.30	0.84	20.50	20.20	21.05 ± 0.07	20.99 ± 0.07	21.15 ± 0.07	21.57 ± 0.07	152.8 ± 13.7	B03-173
BX1132	12 36 03.91	62 15 08.3	...	:2.112	GAL	24.41	0.45	0.98	...	...	22.72 ± 0.07	22.64 ± 0.07	22.53 ± 0.13	...	...	
BX1140	12 36 08.51	62 14 48.0	1.487	...	GAL	24.69	0.10	0.36	...	...	22.62 ± 0.08	22.74 ± 0.12	22.71 ± 0.32	...	9.1 ± 2.9	
BX1145	12 36 10.12	62 14 49.2	...	2.325	GAL	25.40	0.17	0.51	...	...	24.13 ± 0.15	24.23 ± 0.15	...	...	...	
BX1157	12 36 18.30	62 14 09.1	2.083	2.078	GAL	24.14	0.14	0.34	...	...	21.99 ± 0.07	22.00 ± 0.07	21.62 ± 0.16	21.84 ± 0.22	...	
BX1161	12 36 59.39	62 09 21.9	...	1.891	GAL	23.71	0.37	0.59	...	...	21.85 ± 0.07	21.87 ± 0.07	22.24 ± 0.15	22.47 ± 0.19	23.3 ± 5.3	
BX1164	12 36 24.20	62 13 32.6	2.598	2.588	GAL	24.49	0.22	0.85	>25.0	>24.4	24.05 ± 0.16	24.43 ± 0.21	...	...	...	
BX1166	12 36 20.32	62 14 04.9	1.334	...	GAL	24.54	0.09	0.30	22.95	23.13	23.28 ± 0.18	23.55 ± 0.35	...	...	12.5 ± 3.6	
BX1169	12 36 28.27	62 13 15.3	...	1.871	GAL	23.82	0.14	0.43	23.04	22.30	22.47 ± 0.07	22.45 ± 0.07	22.54 ± 0.21	23.14 ± 0.33	40.7 ± 7.7	
BX1170	12 36 31.94	62 12 51.8	2.445	2.441	GAL	24.26	0.35	1.04	23.23	22.58	22.38 ± 0.07	22.49 ± 0.12	22.06 ± 0.30	...	32.9 ± 6.1	
BX1172	12 36 54.35	62 10 18.3	2.811	2.802	GAL	24.50	0.55	1.19	>25.0	>24.4	24.05 ± 0.24	24.31 ± 0.23	...	...	...	S03-D2
BX1174	12 36 47.82	62 11 06.1	2.349	...	GAL	24.37	0.19	0.49	24.40	23.72	23.07 ± 0.17	23.36 ± 0.24	...	...	...	
BX1178	12 36 33.52	62 12 51.8	0.000	0.000	STAR	23.23	0.01	0.42	23.38	22.64	24.01 ± 0.24	...	...	...	...	
BX1183	12 37 08.51	62 08 54.7	2.043	:2.039	GAL	24.67	0.37	1.00	...	...	23.25 ± 0.15	23.51 ± 0.34	...	...	...	
BX1185	12 36 12.60	62 15 30.0	2.207	2.203	GAL	24.99	0.47	0.96	...	...	22.54 ± 0.07	22.46 ± 0.08	22.41 ± 0.15	22.52 ± 0.19	44.1 ± 6.8	
BX1186	12 36 13.20	62 15 26.2	...	2.079	GAL	25.02	0.22	0.53	...	...	24.66 ± 0.25	24.53 ± 0.34	...	...	...	

TABLE 2—*Continued*

Name	α (J2000.0)	δ (J2000.0)	z_{em}[a]	z_{abs}[b]	Type[c]	$\mathcal{R}$[d] (mag)	$G-\mathcal{R}$ (mag)	U_n-G[e] (mag)	J[f] (mag)	K_s[f] (mag)	$m_{3.6\,\mu m}$ (mag)	$m_{4.5\,\mu m}$ (mag)	$m_{5.8\,\mu m}$ (mag)	$m_{8.0\,\mu m}$ (mag)	$f_{24\,\mu m}$ (μJy)	Notes[g]
BX1192.....	12 36 16.83	62 15 14.3	...	1.996	GAL	24.22	0.15	0.86	...	...	21.52 ± 0.07	21.56 ± 0.07	21.47 ± 0.15	21.67 ± 0.22	111.6 ± 10.7	
BX1197.....	12 36 18.89	62 15 06.8	2.599	2.587	GAL	24.13	0.17	0.80	>25.0	>24.4	22.73 ± 0.12	22.76 ± 0.17	...	...	31.9 ± 6.8	
BX1201.....	12 36 14.13	62 15 41.8	...	2.000	GAL	24.00	0.18	0.71	...	...	22.94 ± 0.07	22.99 ± 0.07	23.04 ± 0.27	...	29.0 ± 5.5	
BX1204.....	12 36 21.73	62 14 52.6	2.209	2.200	GAL	24.27	0.32	1.13	23.27	22.38	22.51 ± 0.07	22.62 ± 0.07	22.76 ± 0.15	23.21 ± 0.28	15.8 ± 4.4	
BX1208.....	12 36 41.67	62 12 38.7	2.589	...	GAL	24.44	0.30	0.79	23.66	23.99	23.76 ± 0.13	24.17 ± 0.32	...	...	...	
BX1209.....	12 36 37.07	62 13 11.8	0.348	...	GAL	24.63	0.30	0.88	>25.0	23.07	23.96 ± 0.12	23.93 ± 0.13	...	...	13.1 ± 5.4	
BX1214.....	12 36 44.65	62 12 27.2	...	:1.879	GAL	23.99	0.23	0.60	22.67	22.10	22.05 ± 0.07	21.96 ± 0.07	21.97 ± 0.08	22.39 ± 0.14	46.9 ± 7.0	
BX1217.....	12 37 08.47	62 09 47.1	...	:2.170	GAL	24.73	0.27	0.89	23.40	22.82	23.23 ± 0.07	23.24 ± 0.09	23.27 ± 0.30	23.44 ± 0.33	...	
BX1218.....	12 36 41.69	62 12 58.0	...	:2.054	GAL	23.88	0.11	0.35	23.23	22.50	22.40 ± 0.07	22.40 ± 0.12	22.67 ± 0.19	22.97 ± 0.33	26.2 ± 5.3	
BX1220.....	12 36 30.85	62 14 18.2	0.136	0.136	GAL	24.86	0.41	0.81	23.51	22.45	21.92 ± 0.07	21.91 ± 0.07	21.99 ± 0.07	22.56 ± 0.13	...	
BX1222.....	12 37 02.99	62 10 34.1	2.446	2.438	GAL	24.53	0.26	0.75	>25.0	24.14	24.43 ± 0.35	24.41 ± 0.32	...	...	...	S03-MD18
BX1223.....	12 36 18.22	62 15 51.6	:1.865	...	GAL	25.07	0.25	0.48	23.55	21.81	21.17 ± 0.07	20.92 ± 0.07	20.51 ± 0.07	20.79 ± 0.14	307.4 ± 17.6	DRG
BX1228.....	12 36 20.19	62 15 40.6	1.999	1.995	GAL	24.03	0.39	0.65	23.12	23.33	22.94 ± 0.08	23.10 ± 0.11	23.05 ± 0.22	...	14.7 ± 4.1	
BX1229.....	12 36 33.23	62 14 11.0	1.343	1.343	GAL	23.80	0.12	0.36	23.06	22.57	22.42 ± 0.07	22.40 ± 0.09	22.31 ± 0.22	22.34 ± 0.28	48.4 ± 9.4	
BX1233.....	12 36 36.76	62 13 51.3	2.856	...	GAL	24.67	0.37	0.86	>25.0	23.37	22.75 ± 0.07	22.61 ± 0.07	22.20 ± 0.09	...	...	S03-D12; DRG
BX1238.....	12 36 54.39	62 11 55.4	...	2.261	GAL	24.57	0.30	0.65	24.00	23.33	22.97 ± 0.07	22.91 ± 0.07	23.21 ± 0.20	...	...	
BX1240.....	12 37 06.77	62 10 23.1	...	2.282	GAL	24.01	0.14	0.68	24.06	23.63	23.19 ± 0.11	23.19 ± 0.17	...	...	...	
BX1243.....	12 37 06.66	62 10 35.2	...	:2.037	GAL	23.99	0.27	0.52	23.21	22.99	22.68 ± 0.07	22.71 ± 0.15	22.67 ± 0.22	...	...	
BX1244.....	12 37 02.55	62 11 05.0	...	1.012	GAL	23.68	0.07	0.27	>25.0	>24.4	22.35 ± 0.09	22.48 ± 0.23	22.70 ± 0.32	...	35.7 ± 6.2	
BX1245.....	12 36 16.28	62 16 30.4	2.097	2.089	GAL	23.82	−0.05	0.34	...	...	22.91 ± 0.08	22.91 ± 0.11	...	...	18.8 ± 4.6	
BX1250.....	12 36 32.11	62 14 50.9	1.856	1.853	GAL	24.68	0.04	0.40	24.06	23.39	22.86 ± 0.07	22.86 ± 0.07	22.95 ± 0.13	...	...	
BX1252.....	12 37 07.71	62 10 37.6	...	2.931	GAL	24.12	0.60	1.57	24.56	23.72	23.53 ± 0.21	...	...	...	...	
BX1253.....	12 36 23.62	62 15 55.9	...	1.933	GAL	24.51	0.18	0.38	>25.0	>24.4	22.49 ± 0.07	22.53 ± 0.07	23.13 ± 0.20	23.18 ± 0.33	...	
BX1260.....	12 37 13.31	62 10 14.9	...	:1.714	GAL	24.98	0.50	1.02	22.97	21.60	21.51 ± 0.07	21.45 ± 0.07	21.34 ± 0.08	21.83 ± 0.11	105.7 ± 10.4	
BX1264.....	12 37 09.38	62 10 46.3	2.942	...	GAL	24.76	0.14	0.80	>25.0	23.75	...	...	...	...	...	S03-oMD24
BX1265.....	12 36 33.35	62 15 04.4	2.437	2.431	GAL	23.93	0.17	1.02	24.27	22.74	23.20 ± 0.07	23.27 ± 0.07	23.42 ± 0.26	23.33 ± 0.36	...	S03-oMD51; DRG
BX1267.....	12 36 22.67	62 16 21.6	1.996	1.996	GAL	23.90	0.13	0.51	22.84	22.17	23.45 ± 0.30	...	...	...	48.7 ± 7.2	
BX1269.....	12 37 10.37	62 10 49.2	...	2.275	GAL	23.53	0.45	1.00	22.97	21.96	21.85 ± 0.07	21.78 ± 0.08	21.77 ± 0.20	22.15 ± 0.22	89.1 ± 9.5	
BX1270.....	12 36 51.42	62 13 00.6	0.089	0.089	GAL	22.93	0.28	0.95	22.81	22.89	23.97 ± 0.07	24.35 ± 0.10	...	...	...	
BX1274.....	12 37 11.35	62 10 44.2	2.599	2.594	GAL	24.29	0.25	0.93	24.02	23.87	22.80 ± 0.16	23.02 ± 0.24	...	...	26.6 ± 5.2	
BX1277.....	12 37 18.60	62 09 55.5	...	2.268	GAL	23.87	0.14	0.61	22.89	23.08	23.11 ± 0.07	23.28 ± 0.13	...	...	27.0 ± 5.8	
BX1279.....	12 36 19.45	62 17 01.1	0.995	...	GAL	24.79	−0.19	0.19	>25.0	>24.4	23.79 ± 0.18	24.15 ± 0.17	...	...	40.7 ± 8.9	
BX1281.....	12 37 03.39	62 11 53.5	...	2.410	GAL	25.16	0.32	0.70	>25.0	23.89	23.84 ± 0.15	24.11 ± 0.26	...	...	13.4 ± 3.9	S03-D8
BX1283.....	12 37 16.29	62 10 23.3	...	2.427	GAL	24.59	0.24	0.60	23.46	22.72	22.69 ± 0.08	22.69 ± 0.08	23.31 ± 0.21	23.18 ± 0.36	...	
BX1284.....	12 36 44.08	62 14 09.9	2.276	2.270	GAL	24.37	0.01	0.61	23.77	22.97	23.28 ± 0.12	23.33 ± 0.17	23.10 ± 0.28	...	...	
BX1287.....	12 36 20.64	62 16 57.9	...	1.675	GAL	23.05	0.05	0.34	22.17	22.58	22.60 ± 0.07	22.50 ± 0.08	22.68 ± 0.12	23.27 ± 0.36	35.1 ± 6.4	
BX1288.....	12 37 11.14	62 11 04.5	2.301	...	GAL	24.16	0.10	0.58	23.29	23.50	23.15 ± 0.08	23.31 ± 0.10	23.57 ± 0.29	...	...	
BX1289.....	12 36 33.67	62 15 32.9	...	2.488	GAL	24.15	0.34	1.16	23.47	22.64	22.76 ± 0.07	22.77 ± 0.07	22.90 ± 0.13	22.91 ± 0.16	18.8 ± 4.5	
BX1290.....	12 36 35.55	62 15 21.8	2.980	...	GAL	24.69	0.39	0.79	>25.0	>24.4	23.81 ± 0.28	24.16 ± 0.30	...	...	...	S03-oMD54
BX1291.....	12 37 00.11	62 12 25.2	...	2.052	GAL	23.56	0.30	0.80	23.49	23.17	23.05 ± 0.14	23.15 ± 0.12	23.19 ± 0.24	23.71 ± 0.34	22.4 ± 5.3	
BX1293.....	12 36 46.52	62 14 07.5	0.128	...	GAL	24.22	0.33	0.67	23.53	23.43	21.07 ± 0.07	21.09 ± 0.07	21.06 ± 0.07	20.79 ± 0.07	199.2 ± 14.5	
BX1296.....	12 36 20.91	62 17 09.5	1.989	1.988	GAL	24.15	0.26	0.59	22.82	21.75	21.19 ± 0.07	20.96 ± 0.07	20.67 ± 0.09	21.00 ± 0.14	263.7 ± 16.4	
BX1297.....	12 37 13.08	62 11 02.2	...	2.274	GAL	24.53	0.35	0.82	23.25	22.00	21.89 ± 0.07	21.85 ± 0.07	21.76 ± 0.12	22.19 ± 0.23	...	
BX1299.....	12 36 53.24	62 13 22.2	1.654	1.649	GAL	23.49	0.36	0.61	23.38	22.32	22.94 ± 0.08	22.96 ± 0.07	23.49 ± 0.26	...	18.7 ± 5.1	
BX1300.....	12 36 54.76	62 13 14.7	:2.288	:2.288	GAL	24.55	0.21	0.65	24.08	23.34	22.93 ± 0.14	23.06 ± 0.19	...	...	...	
BX1303.....	12 37 11.20	62 11 18.7	2.305	2.304	GAL	24.72	0.11	0.81	24.24	22.85	23.55 ± 0.18	23.35 ± 0.14	...	...	15.1 ± 4.0	DRG
BX1305.....	12 36 50.12	62 14 01.0	2.238	2.231	GAL	24.77	0.14	0.72	23.35	23.00	22.80 ± 0.09	22.76 ± 0.11	22.68 ± 0.26	22.76 ± 0.31	73.1 ± 8.9	

TABLE 2—*Continued*

Name	α (J2000.0)	δ (J2000.0)	z_{em}[a]	z_{abs}[b]	Type[c]	$\mathcal{R}$[d] (mag)	$G-\mathcal{R}$ (mag)	U_n-G[e] (mag)	J[f] (mag)	K_s[f] (mag)	$m_{3.6\,\mu m}$ (mag)	$m_{4.5\,\mu m}$ (mag)	$m_{5.8\,\mu m}$ (mag)	$m_{8.0\,\mu m}$ (mag)	$f_{24\,\mu m}$ (μJy)	Notes[g]
BX1307.....	12 36 48.33	62 14 16.7	...	2.002	GAL	23.30	0.20	0.74	22.69	21.83	21.69 ± 0.07	21.61 ± 0.07	21.34 ± 0.09	21.44 ± 0.26	145.5 ± 12.2	
BX1311.....	12 36 30.54	62 16 26.1	2.490	2.479	GAL	23.29	0.21	0.81	22.94	22.30	22.65 ± 0.10	22.74 ± 0.12	22.60 ± 0.17	...	24.0 ± 5.1	
BX1312.....	12 37 02.27	62 12 43.2	0.107	0.107	GAL	22.72	0.46	1.04	22.32	22.71	23.86 ± 0.16	...	...	...	45.4 ± 9.2	
BX1313.....	12 37 04.04	62 12 33.8	2.637	2.632	GAL	24.31	0.42	0.99	>25.0	>24.4	23.68 ± 0.07	23.71 ± 0.25	...	...	...	
BX1315.....	12 36 30.10	62 16 35.9	...	1.671	GAL	23.77	0.19	0.41	22.62	22.06	21.79 ± 0.07	21.75 ± 0.07	21.91 ± 0.07	22.05 ± 0.17	64.8 ± 8.2	
BX1316.....	12 37 20.70	62 10 40.7	2.088	...	GAL	24.26	0.20	0.55	23.16	22.41	22.04 ± 0.07	21.99 ± 0.09	21.79 ± 0.22	...	...	
BX1317.....	12 36 25.36	62 17 08.0	1.792	1.787	GAL	23.28	0.16	0.41	22.44	21.78	22.26 ± 0.07	22.25 ± 0.07	22.32 ± 0.14	22.50 ± 0.17	53.9 ± 7.7	
BX1319.....	12 37 04.26	62 12 39.5	1.109	1.109	GAL	23.33	0.31	0.62	22.54	21.82	21.34 ± 0.07	21.23 ± 0.07	21.17 ± 0.07	21.46 ± 0.09	102.1 ± 10.4	
BX1321.....	12 36 48.31	62 14 26.5	0.139	...	...	19.22	0.32	0.91	18.72	18.46	19.37 ± 0.07	19.74 ± 0.07	19.73 ± 0.07	17.68 ± 0.07	434.8 ± 21.4	B03-251
BX1322.....	12 37 06.54	62 12 24.9	2.449	2.438	GAL	23.72	0.31	0.57	24.01	22.77	23.25 ± 0.14	23.28 ± 0.16	...	...	31.9 ± 6.0	
BX1324.....	12 37 12.95	62 11 44.5	1.821	1.815	GAL	24.38	0.46	1.03	22.85	22.15	21.79 ± 0.07	21.70 ± 0.07	21.90 ± 0.13	22.09 ± 0.16	143.0 ± 12.2	
BX1326.....	12 36 35.71	62 16 14.9	2.984	...	GAL	24.49	0.40	0.73	>25.0	23.90	23.81 ± 0.12	24.17 ± 0.18	...	...	...	
BX1327.....	12 36 57.51	62 13 44.2	2.209	...	GAL	24.05	0.21	0.44	23.13	22.51	22.92 ± 0.07	23.00 ± 0.07	22.98 ± 0.16	23.45 ± 0.23	23.3 ± 5.2	
BX1329.....	12 36 54.62	62 14 07.7	...	:1.987	GAL	24.69	−0.04	0.45	23.95	23.79	24.46 ± 0.25	...	...	...	8.2 ± 2.5	
BX1330.....	12 36 48.91	62 14 50.9	...	2.363	GAL	23.73	0.05	0.61	23.66	22.72	22.91 ± 0.07	22.95 ± 0.07	22.86 ± 0.11	...	24.8 ± 5.4	
BX1332.....	12 37 17.13	62 11 39.9	2.218	2.209	GAL	23.64	0.32	0.92	23.35	22.50	22.50 ± 0.08	22.53 ± 0.11	22.41 ± 0.13	...	29.7 ± 5.6	
BX1334.....	12 36 46.64	62 15 17.0	3.371	...	GAL	25.11	0.46	1.19	>25.0	23.22	...	...	...	...	...	S03-M28; DRG
BX1335.....	12 36 44.69	62 15 31.2	...	:2.453	AGN?	25.15	0.28	0.94	23.74	22.84	22.90 ± 0.07	22.89 ± 0.07	22.67 ± 0.15	22.88 ± 0.15	19.3 ± 4.6	
BX1339.....	12 36 25.09	62 17 56.8	1.993	1.984	GAL	24.60	−0.05	0.48	...	...	23.06 ± 0.09	23.03 ± 0.12	22.63 ± 0.31	...	...	
BX1343.....	12 37 08.77	62 12 57.8	...	2.268	GAL	23.98	0.17	0.82	22.88	22.57	22.45 ± 0.07	22.51 ± 0.07	22.45 ± 0.34	...	21.0 ± 5.4	
BX1348.....	12 37 05.84	62 13 29.3	1.923	1.919	GAL	24.76	0.05	0.29	23.84	23.89	23.88 ± 0.23	...	...	...	24.8 ± 5.7	
BX1349.....	12 36 57.27	62 14 29.7	...	1.873	GAL	24.29	0.41	0.74	22.93	22.18	21.61 ± 0.07	21.45 ± 0.07	21.49 ± 0.09	21.68 ± 0.09	104.8 ± 10.4	
BX1350.....	12 37 05.50	62 13 34.6	...	:2.830	GAL	24.56	0.45	1.14	>25.0	>24.4	...	...	...	...	...	S03-MD37
BX1351.....	12 36 59.40	62 14 04.7	0.089	0.089	GAL	20.17	0.45	1.01	19.69	19.83	21.53 ± 0.07	21.90 ± 0.07	21.98 ± 0.07	21.55 ± 0.07	...	
BX1353.....	12 36 31.15	62 17 39.9	...	:2.505	GAL	24.28	0.24	0.61	22.92	22.03	21.82 ± 0.07	21.75 ± 0.07	21.92 ± 0.20	22.14 ± 0.22	65.7 ± 8.4	
BX1354.....	12 37 17.25	62 12 20.3	2.088	2.088	GAL	24.98	−0.10	0.38	>25.0	>24.4	24.50 ± 0.20	...	...	...	...	
BX1355.....	12 36 43.16	62 16 20.1	...	2.307	GAL	24.09	0.13	1.07	23.77	22.98	22.34 ± 0.07	22.53 ± 0.11	22.94 ± 0.15	...	...	
BX1358.....	12 36 59.46	62 14 27.7	2.943	...	GAL	24.83	0.49	1.45	>25.0	23.73	24.11 ± 0.12	24.25 ± 0.11	...	...	...	
BX1361.....	12 36 30.47	62 17 53.9	...	:1.849	GAL	25.48	−0.04	0.22	>25.0	23.43	24.22 ± 0.20	...	...	...	...	DRG
BX1362.....	12 36 42.57	62 16 29.4	...	1.664	GAL	24.55	0.05	0.28	23.56	22.83	22.08 ± 0.07	22.34 ± 0.07	...	...	...	
BX1363.....	12 37 27.40	62 11 12.7	...	2.297	GAL	23.82	0.33	0.76	22.89	22.15	22.58 ± 0.07	22.59 ± 0.07	22.52 ± 0.14	22.76 ± 0.29	58.8 ± 7.8	
BX1364.....	12 37 23.74	62 11 41.2	...	2.183	GAL	24.27	0.22	0.74	23.56	22.82	22.65 ± 0.07	22.64 ± 0.12	22.78 ± 0.19	23.14 ± 0.31	11.5 ± 3.7	
BX1368.....	12 36 48.24	62 15 56.2	2.446	2.440	GAL	23.79	0.30	0.96	23.34	22.45	22.35 ± 0.07	22.60 ± 0.16	22.43 ± 0.29	22.40 ± 0.33	71.0 ± 8.7	
BX1371.....	12 37 16.57	62 12 45.2	0.947	...	GAL	24.23	0.30	0.95	23.84	23.79	24.49 ± 0.24	24.95 ± 0.35	...	...	...	
BX1374.....	12 36 57.90	62 15 07.0	0.116	0.116	GAL	23.80	0.26	0.88	23.27	23.41	24.13 ± 0.13	...	...	...	...	
BX1376.....	12 36 52.96	62 15 45.5	2.434	2.426	GAL	24.48	0.01	0.70	24.05	23.95	23.93 ± 0.09	24.05 ± 0.18	...	...	...	
BX1378.....	12 37 02.02	62 14 43.4	...	1.971	GAL	23.90	0.33	0.66	23.14	22.75	22.42 ± 0.07	22.40 ± 0.07	22.43 ± 0.10	23.15 ± 0.18	29.4 ± 5.5	
BX1387.....	12 36 56.32	62 15 52.4	...	2.324	GAL	24.77	0.17	0.61	23.72	23.89	23.61 ± 0.08	23.60 ± 0.08	23.40 ± 0.31	...	15.2 ± 4.5	
BX1388.....	12 36 44.84	62 17 15.8	...	2.032	GAL	24.55	0.27	0.99	22.63	21.77	21.55 ± 0.07	21.43 ± 0.07	21.23 ± 0.07	21.54 ± 0.13	151.7 ± 12.3	
BX1391.....	12 37 13.87	62 13 54.9	...	1.906	GAL	24.06	0.35	0.57	23.14	22.98	22.46 ± 0.07	22.45 ± 0.07	22.52 ± 0.09	23.19 ± 0.19	...	
BX1392.....	12 37 25.92	62 12 06.4	0.089	...	GAL	21.58	0.37	0.94	21.27	21.23	22.48 ± 0.07	22.85 ± 0.07	23.35 ± 0.30	23.04 ± 0.15	...	
BX1397.....	12 37 04.12	62 15 09.8	...	2.133	GAL	24.12	0.14	0.76	22.85	22.69	22.47 ± 0.07	22.36 ± 0.07	22.30 ± 0.12	22.50 ± 0.16	30.2 ± 5.9	
BX1399.....	12 37 18.30	62 13 32.6	...	2.033	GAL	25.22	0.23	0.73	23.91	23.49	22.73 ± 0.10	22.84 ± 0.13	22.51 ± 0.31	...	20.9 ± 5.0	
BX1400.....	12 37 06.09	62 15 01.5	:3.239	...	GAL	23.77	0.52	1.21	23.17	23.41	23.79 ± 0.09	24.10 ± 0.11	...	...	...	
BX1401.....	12 37 02.93	62 15 22.5	...	2.481	GAL	23.47	0.41	0.87	22.38	21.73	21.76 ± 0.07	21.57 ± 0.07	21.35 ± 0.10	21.60 ± 0.13	41.2 ± 6.8	
BX1403.....	12 37 25.12	62 12 49.5	...	:1.706	GAL	24.63	0.32	0.52	>25.0	>24.4	22.85 ± 0.10	22.82 ± 0.16	...	...	15.4 ± 4.3	
BX1408.....	12 36 57.40	62 16 18.2	...	2.482	GAL	24.83	0.64	1.47	24.13	22.68	22.49 ± 0.07	22.38 ± 0.07	22.28 ± 0.11	22.63 ± 0.12	31.4 ± 6.1	S03-MD40; DRG

TABLE 2—*Continued*

Name	α (J2000.0)	δ (J2000.0)	z_{em}[a]	z_{abs}[b]	Type[c]	$\mathcal{R}$[d] (mag)	$G-\mathcal{R}$ (mag)	U_n-G[e] (mag)	J[f] (mag)	K_s[f] (mag)	$m_{3.6\,\mu m}$ (mag)	$m_{4.5\,\mu m}$ (mag)	$m_{5.8\,\mu m}$ (mag)	$m_{8.0\,\mu m}$ (mag)	$f_{24\,\mu m}$ (μJy)	Notes[g]
BX1409.....	12 36 47.41	62 17 28.7	...	2.237	GAL	24.66	0.49	1.17	23.28	21.89	22.23 ± 0.07	22.22 ± 0.08	22.10 ± 0.18	22.34 ± 0.20	52.1 ± 7.4	DRG
BX1420.....	12 36 50.87	62 17 12.4	...	2.133	GAL	23.79	0.45	1.01	22.84	22.34	22.06 ± 0.07	22.13 ± 0.07	...	...	18.5 ± 4.5	
BX1425.....	12 37 17.96	62 14 17.6	...	1.864	GAL	24.65	0.02	0.28	23.44	23.66	23.30 ± 0.07	23.28 ± 0.07	23.50 ± 0.33	...	...	
BX1427.....	12 37 33.28	62 12 33.8	...	2.548	GAL	24.54	0.39	0.85	...	...	22.98 ± 0.08	22.97 ± 0.08	22.82 ± 0.21	...	8.3 ± 2.2	
BX1431.....	12 36 58.48	62 16 45.5	2.006	1.996	GAL	24.00	0.09	0.45	>25.0	23.13	23.11 ± 0.16	23.25 ± 0.34	...	...	...	DRG
BX1434.....	12 37 16.80	62 14 38.8	...	1.994	GAL	24.49	0.26	0.51	23.62	23.21	23.14 ± 0.19	23.18 ± 0.27	...	...	...	
BX1439.....	12 36 53.66	62 17 24.3	2.191	2.186	GAL	23.90	0.26	0.79	22.78	21.54	21.91 ± 0.07	21.82 ± 0.09	21.82 ± 0.12	22.05 ± 0.21	85.3 ± 9.4	
BX1443.....	12 36 44.87	62 18 37.9	...	1.684	GAL	23.33	0.31	0.57	...	...	20.85 ± 0.07	20.67 ± 0.07	20.81 ± 0.07	20.93 ± 0.07	194.0 ± 14.0	
BX1446.....	12 36 43.42	62 18 55.3	2.326	2.315	GAL	24.21	0.16	0.71	...	...	23.08 ± 0.13	23.00 ± 0.15	...	...	...	
BX1451.....	12 37 13.22	62 15 31.7	...	2.245	GAL	24.58	0.40	0.86	23.54	22.84	22.37 ± 0.10	22.23 ± 0.08	22.36 ± 0.28	22.47 ± 0.28	36.0 ± 6.1	
BX1458.....	12 37 26.95	62 14 03.6	...	1.864	GAL	24.84	0.35	0.68	23.19	23.05	22.63 ± 0.13	22.78 ± 0.23	...	...	52.4 ± 7.5	
BX1460.....	12 36 56.80	62 17 25.5	3.137	3.131	GAL	24.70	0.41	1.30	24.39	23.68	23.30 ± 0.12	23.72 ± 0.21	23.18 ± 0.35	...	...	
BX1461.....	12 36 49.54	62 18 33.2	2.107	2.107	GAL	24.77	0.23	0.63	...	...	23.54 ± 0.11	23.48 ± 0.08	...	23.77 ± 0.36	...	
BX1476.....	12 37 19.55	62 15 20.8	1.930	1.927	GAL	25.19	0.15	0.37	>25.0	>24.4	22.46 ± 0.07	23.04 ± 0.11	...	...	...	
BX1479.....	12 37 15.42	62 16 03.9	2.383	2.371	GAL	24.39	0.16	0.79	23.77	23.12	23.03 ± 0.12	23.08 ± 0.17	22.68 ± 0.34	...	10.9 ± 3.6	
BX1480.....	12 37 25.43	62 14 56.2	...	2.545	GAL	24.28	0.53	1.13	24.06	23.32	22.65 ± 0.08	22.54 ± 0.09	22.52 ± 0.19	22.80 ± 0.28	18.3 ± 4.3	
BX1485.....	12 37 28.12	62 14 39.9	...	2.548	GAL	23.29	0.35	0.96	22.96	22.02	21.36 ± 0.07	21.32 ± 0.09	21.19 ± 0.16	21.30 ± 0.17	315.9 ± 17.9	
BX1495.....	12 37 24.88	62 15 22.4	2.251	2.244	GAL	24.98	0.20	0.73	>25.0	23.32	23.48 ± 0.23	23.40 ± 0.27	...	...	...	DRG
BX1501.....	12 37 41.58	62 13 22.2	1.879	1.875	GAL	23.78	0.16	0.46	...	...	22.19 ± 0.09	22.16 ± 0.09	22.28 ± 0.21	22.74 ± 0.36	43.3 ± 7.1	
BX1504.....	12 37 41.90	62 13 33.7	2.869	2.858	GAL	24.34	0.52	1.42	...	...	23.75 ± 0.22	23.71 ± 0.13	23.55 ± 0.34	...	...	
BX1505.....	12 36 59.12	62 18 35.8	1.012	...	GAL	24.49	0.11	0.34	...	...	22.93 ± 0.10	22.94 ± 0.14	22.57 ± 0.32	22.00 ± 0.21	256.2 ± 16.2	
BX1510.....	12 37 27.13	62 15 28.3	...	:2.072	GAL	24.90	0.15	0.57	23.54	23.98	23.52 ± 0.15	23.50 ± 0.25	...	...	...	
BX1514.....	12 37 14.93	62 16 59.8	...	2.135	GAL	24.90	0.29	0.56	23.48	>24.4	22.68 ± 0.09	22.51 ± 0.08	22.96 ± 0.34	22.80 ± 0.25	22.2 ± 5.0	
BX1525.....	12 37 24.15	62 16 11.6	1.689	1.689	GAL	24.15	0.28	0.56	22.44	21.56	21.59 ± 0.07	21.41 ± 0.07	21.55 ± 0.12	21.60 ± 0.11	120.4 ± 11.1	
BX1529.....	12 37 01.68	62 18 48.6	0.232	...	GAL	24.31	0.27	0.51	...	...	...	...	...	...	...	
BX1530.....	12 37 22.85	62 16 27.6	...	2.421	GAL	24.40	0.25	0.84	24.18	23.19	23.41 ± 0.15	23.33 ± 0.17	...	22.83 ± 0.33	...	
BX1535.....	12 37 07.18	62 18 30.1	...	2.299	GAL	24.31	0.33	0.97	...	...	23.18 ± 0.07	23.17 ± 0.09	23.27 ± 0.35	23.46 ± 0.26	...	
BX1542.....	12 36 55.06	62 20 05.2	1.018	...	GAL	24.72	0.11	0.31	...	...	23.34 ± 0.19	23.70 ± 0.32	...	...	...	
BX1544.....	12 37 14.85	62 17 47.3	...	:2.486	GAL	24.27	0.24	1.13	...	...	...	...	...	...	...	
BX1548.....	12 37 00.49	62 19 30.3	0.223	...	GAL	23.79	0.46	0.89	...	...	23.95 ± 0.17	24.71 ± 0.31	...	...	...	
BX1557.....	12 37 27.17	62 16 31.7	...	1.776	GAL	23.74	0.31	0.80	22.99	23.00	21.64 ± 0.07	21.73 ± 0.07	21.29 ± 0.08	22.85 ± 0.20	167.9 ± 13.0	
BX1559.....	12 37 29.41	62 15 40.1	...	2.408	GAL	24.19	0.07	0.59	23.84	23.53	23.10 ± 0.28	23.08 ± 0.18	...	...	85.8 ± 9.7	
BX1564.....	12 37 23.47	62 17 20.0	...	2.218	GAL	23.28	0.27	1.01	22.21	21.44	21.77 ± 0.07	21.69 ± 0.07	21.57 ± 0.10	21.98 ± 0.20	74.8 ± 8.9	
BX1567.....	12 37 23.17	62 17 23.9	...	2.225	GAL	23.50	0.18	1.05	22.31	22.00	21.96 ± 0.07	21.86 ± 0.07	21.79 ± 0.11	22.03 ± 0.19	34.1 ± 6.2	DLA
BX1568.....	12 36 54.06	62 20 48.1	...	1.787	GAL	23.46	0.08	0.44	...	...	22.68 ± 0.08	22.63 ± 0.09	22.68 ± 0.23	23.30 ± 0.26	25.5 ± 5.9	
BX1572.....	12 36 58.51	62 20 29.3	...	1.782	GAL	24.32	0.25	0.59	...	...	23.43 ± 0.07	23.47 ± 0.07	23.63 ± 0.31	...	...	
BX1574.....	12 37 25.95	62 17 10.1	...	1.808	GAL	24.24	0.22	0.66	22.66	22.33	22.00 ± 0.07	21.90 ± 0.07	22.08 ± 0.14	22.12 ± 0.19	55.3 ± 7.6	
BX1579.....	12 37 38.93	62 15 41.0	0.190	...	GAL	22.98	0.38	0.62	...	...	23.65 ± 0.24	24.17 ± 0.26	...	...	58.1 ± 8.1	
BX1586.....	12 37 24.91	62 17 40.8	...	:1.901	GAL	24.44	0.41	0.82	23.54	23.10	23.02 ± 0.17	23.02 ± 0.12	...	...	22.5 ± 5.2	
BX1588.....	12 37 02.54	62 20 20.9	...	2.221	GAL	23.22	0.30	1.17	>25.0	>24.4	21.58 ± 0.07	21.48 ± 0.07	21.24 ± 0.11	21.52 ± 0.20	129.7 ± 11.6	
BX1591.....	12 37 28.21	62 17 22.6	2.050	2.048	GAL	24.45	0.21	0.52	23.03	22.97	23.17 ± 0.08	23.24 ± 0.07	23.49 ± 0.26	...	10.0 ± 2.0	
BX1605.....	12 37 21.51	62 18 30.6	1.977	1.970	GAL	23.89	−0.07	0.19	...	...	23.29 ± 0.07	23.36 ± 0.17	...	...	...	
BX1616.....	12 37 32.75	62 17 27.6	...	2.205	GAL	25.29	0.13	0.35	...	...	23.79 ± 0.30	...	...	...	...	
BX1617.....	12 37 04.16	62 20 50.8	2.323	2.317	GAL	25.15	0.15	0.68	...	...	23.96 ± 0.10	23.99 ± 0.09	...	23.37 ± 0.31	...	
BX1630.....	12 37 25.95	62 18 32.5	2.222	2.217	GAL	24.35	0.03	0.52	...	...	23.40 ± 0.11	23.49 ± 0.07	...	23.54 ± 0.32	...	
BX1636.....	12 37 20.03	62 19 23.1	2.306	2.295	GAL	24.08	0.44	1.16	...	...	21.93 ± 0.07	21.82 ± 0.07	21.66 ± 0.14	21.82 ± 0.27	71.2 ± 8.5	
BX1637.....	12 37 04.82	62 21 11.5	2.487	...	AGN	24.92	−0.01	0.81	...	...	23.38 ± 0.29	22.76 ± 0.21	21.84 ± 0.18	20.93 ± 0.15	109.4 ± 10.8	

TABLE 2—*Continued*

Name	α (J2000.0)	δ (J2000.0)	z_{em}[a]	z_{abs}[b]	Type[c]	$\mathcal{R}$[d] (mag)	$G-\mathcal{R}$ (mag)	U_n-G[e] (mag)	J[f] (mag)	K_s[f] (mag)	$m_{3.6\,\mu m}$ (mag)	$m_{4.5\,\mu m}$ (mag)	$m_{5.8\,\mu m}$ (mag)	$m_{8.0\,\mu m}$ (mag)	$f_{24\,\mu m}$ (μJy)	Notes[g]
BX1641	12 37 08.89	62 20 44.7	1.433	...	GAL	24.20	0.01	0.26	...	...	23.79 ± 0.10	23.93 ± 0.16	...	...	...	
BX1642	12 37 32.40	62 17 50.8	2.010	2.004	GAL	24.29	0.25	0.46	...	...	22.97 ± 0.09	22.95 ± 0.09	...	...	...	
BX1650	12 37 24.11	62 19 04.7	2.100	2.094	GAL	23.24	0.18	0.74	...	...	22.10 ± 0.07	22.05 ± 0.07	21.95 ± 0.11	22.42 ± 0.24	37.5 ± 6.5	
BX1655	12 37 32.30	62 18 16.3	0.157	...	GAL	24.37	0.41	1.21	...	...	24.55 ± 0.09	24.92 ± 0.22	...	...	...	
BX1669	12 37 48.40	62 16 34.8	0.118	...	GAL	23.24	0.35	0.96	...	...	23.22 ± 0.07	23.41 ± 0.07	...	23.44 ± 0.34	...	
BX1676	12 37 36.68	62 18 02.1	0.188	...	GAL	23.49	0.42	0.80	...	...	23.58 ± 0.07	23.81 ± 0.29	...	...	51.0 ± 9.3	
BX1694	12 37 33.82	62 18 46.3	2.009	2.005	GAL	23.66	0.11	0.53	...	...	22.50 ± 0.07	22.58 ± 0.07	22.28 ± 0.11	...	13.8 ± 4.3	
BX1708	12 37 32.65	62 19 10.6	...	1.987	GAL	24.50	0.45	1.00	...	...	21.46 ± 0.07	21.23 ± 0.07	21.03 ± 0.07	21.34 ± 0.08	208.3 ± 14.6	
BX1782	12 36 57.46	62 08 38.0	0.177	0.177	GAL	22.27	0.43	0.75	...	...	22.64 ± 0.15	23.17 ± 0.23	...	...	30.3 ± 5.6	
BX1790	12 36 59.31	62 09 31.2	...	2.990	GAL	23.81	0.62	1.17	22.58	23.20	23.20 ± 0.21	23.09 ± 0.18	...	...	...	
BX1796	12 36 27.51	62 14 18.8	0.089	...	GAL	22.70	0.49	0.70	22.43	22.15	22.43 ± 0.07	22.93 ± 0.07	22.71 ± 0.14	...	...	
BX1805	12 36 38.64	62 14 21.8	0.306	0.306	GAL	22.80	0.48	0.80	21.66	21.10	21.99 ± 0.07	22.37 ± 0.07	22.67 ± 0.09	22.59 ± 0.20	95.2 ± 10.3	
BX1808	12 36 59.54	62 12 14.2	...	:1.943	GAL	24.09	0.43	0.68	23.33	23.38	23.01 ± 0.12	23.29 ± 0.36	...	...	...	
BX1815	12 37 15.22	62 11 02.6	0.000	0.000	STAR	19.64	0.54	1.08	19.48	19.87	21.13 ± 0.07	21.68 ± 0.07	22.08 ± 0.07	22.81 ± 0.14	...	
BX1816	12 36 44.13	62 14 50.7	...	:2.095	GAL	24.25	0.53	0.87	23.16	22.00	21.42 ± 0.07	21.26 ± 0.07	21.25 ± 0.11	21.62 ± 0.21	...	
BX1817	12 36 23.27	62 16 43.2	1.862	1.858	GAL	24.54	0.46	0.76	23.66	22.69	21.65 ± 0.07	21.77 ± 0.09	21.75 ± 0.31	...	43.4 ± 7.4	
BX1820	12 37 19.43	62 11 13.8	...	2.457	GAL	24.11	0.65	1.35	23.07	22.07	21.64 ± 0.07	21.49 ± 0.07	21.27 ± 0.12	21.32 ± 0.08	105.6 ± 10.5	
BX1821	12 37 12.63	62 12 10.4	...	2.590	GAL	24.79	0.60	1.11	23.93	23.54	23.28 ± 0.21	23.44 ± 0.28	22.87 ± 0.33	...	15.1 ± 4.8	
BX1822	12 37 05.74	62 13 03.2	0.109	...	GAL	22.05	0.59	1.14	22.03	21.91	22.78 ± 0.07	23.24 ± 0.07	23.03 ± 0.27	...	...	
BX1823	12 37 15.40	62 12 17.9	...	1.818	GAL	24.65	0.49	0.78	22.24	21.33	20.88 ± 0.07	20.76 ± 0.07	20.78 ± 0.09	21.02 ± 0.14	127.4 ± 11.4	
BX1826	12 37 17.38	62 12 46.8	...	2.929	GAL	24.67	0.52	1.02	23.99	23.78	23.49 ± 0.13	23.52 ± 0.27	...	...	32.0 ± 6.9	
BX1827	12 36 56.63	62 15 19.0	1.988	...	GAL	24.84	0.56	1.12	24.48	23.28	23.42 ± 0.09	23.46 ± 0.13	...	...	...	
BX1828	12 37 16.22	62 13 24.3	...	:2.967	GAL	24.09	0.66	1.40	23.35	23.45	24.06 ± 0.08	24.75 ± 0.19	...	...	...	
BX1833	12 37 11.13	62 14 33.8	0.000	0.000	STAR	22.12	0.59	1.02	22.30	22.01	22.56 ± 0.07	22.91 ± 0.10	...	...	...	
BX1841	12 37 02.63	62 16 33.9	...	2.373	GAL	24.70	0.47	1.04	23.46	23.12	22.57 ± 0.12	22.81 ± 0.10	22.80 ± 0.26	...	...	
BX1848	12 37 25.86	62 14 42.4	2.648	...	GAL	25.05	0.45	0.81	>25.0	>24.4	23.93 ± 0.18	24.32 ± 0.31	...	...	12.4 ± 3.7	
BX1851	12 37 29.99	62 15 59.5	0.215	...	GAL	22.96	0.48	0.72	22.31	22.07	22.44 ± 0.14	22.60 ± 0.12	...	...	...	
BX1856	12 37 22.40	62 17 18.0	0.232	...	GAL	23.03	0.51	0.82	22.51	22.34	23.49 ± 0.12	23.87 ± 0.13	23.82 ± 0.31	23.30 ± 0.28	...	
BX1860	12 37 30.81	62 16 54.7	...	:2.504	GAL	24.80	0.51	0.85	>25.0	23.71	22.73 ± 0.12	22.75 ± 0.12	22.57 ± 0.22	...	29.6 ± 5.7	
BX28	12 37 17.78	62 09 37.8	0.229	...	GAL	23.74	0.61	0.78	23.54	23.11	...	...	22.71 ± 0.09	22.45 ± 0.07	...	
BX82	12 37 05.37	62 10 45.3	1.023	...	GAL	24.41	0.58	0.19	23.29	22.94	23.30 ± 0.13	23.55 ± 0.18	...	...	...	
BX84	12 37 13.74	62 10 42.0	2.166	2.161	GAL	24.15	0.22	0.80	>25.0	>24.4	22.08 ± 0.10	21.98 ± 0.13	21.88 ± 0.27	22.30 ± 0.36	79.0 ± 8.9	
BX150	12 37 14.98	62 12 07.9	2.281	2.273	GAL	24.64	0.54	0.53	>25.0	>24.4	22.34 ± 0.12	22.12 ± 0.12	21.87 ± 0.35	...	46.9 ± 7.0	
BX160	12 37 20.07	62 12 23.0	2.462	2.458	AGN	24.02	0.74	0.92	22.83	21.87	21.52 ± 0.07	21.32 ± 0.07	20.98 ± 0.07	20.95 ± 0.09	142.2 ± 12.0	
BX184	12 37 19.28	62 13 00.6	1.998	...	GAL	24.22	0.70	0.99	23.42	23.46	22.80 ± 0.07	22.95 ± 0.25	...	...	...	
BX274	12 36 53.60	62 15 25.0	0.000	0.000	STAR	18.57	0.33	0.96	18.48	18.96	20.07 ± 0.07	20.58 ± 0.07	21.05 ± 0.07	21.76 ± 0.10	...	
BX283	12 37 24.35	62 15 58.3	0.129	...	GAL	23.41	0.44	0.84	>25.0	>24.4	24.55 ± 0.19	24.75 ± 0.33	...	...	...	
BX289	12 37 00.47	62 16 04.9	0.941	...	GAL	24.49	0.69	0.22	23.39	23.25	23.35 ± 0.07	23.87 ± 0.12	...	...	106.6 ± 10.8	
BX305	12 36 37.13	62 16 28.7	...	2.482	GAL	24.28	0.79	1.30	23.63	21.96	22.03 ± 0.07	22.00 ± 0.07	21.90 ± 0.10	21.71 ± 0.10	69.4 ± 8.6	DRG
BX308	12 37 02.66	62 16 34.0	...	2.376	GAL	24.87	0.46	0.95	>25.0	>24.4	22.53 ± 0.10	22.75 ± 0.12	22.79 ± 0.24	...	...	
BX313	12 36 29.66	62 16 45.1	...	2.323	GAL	24.34	0.42	0.60	>25.0	>24.4	22.65 ± 0.07	22.58 ± 0.07	22.36 ± 0.12	22.55 ± 0.16	48.8 ± 7.1	
BX341	12 36 22.26	62 17 30.9	2.117	2.117	GAL	23.56	0.71	0.27	23.77	22.73	22.47 ± 0.07	22.58 ± 0.09	...	22.91 ± 0.26	...	
BM1008	12 35 47.95	62 12 52.3	1.801	1.798	GAL	23.58	0.24	0.25	...	...	22.68 ± 0.07	22.60 ± 0.08	23.20 ± 0.31	22.90 ± 0.33	27.5 ± 5.8	
BM1010	12 36 08.08	62 10 44.7	...	1.346	GAL	24.03	0.16	0.18	...	...	22.69 ± 0.07	22.88 ± 0.12	...	...	37.4 ± 6.4	
BM1011	12 35 51.57	62 12 42.0	1.677	1.677	GAL	23.90	0.28	0.33	...	...	22.21 ± 0.07	22.25 ± 0.07	22.40 ± 0.10	23.06 ± 0.23	20.9 ± 5.2	
BM1017	12 36 11.72	62 10 39.3	...	:2.371	GAL	24.58	0.17	0.20	...	...	22.99 ± 0.12	22.91 ± 0.21	...	...	20.6 ± 5.3	
BM1030	12 35 55.26	62 14 01.2	1.143	1.142	GAL	24.29	0.20	0.37	...	...	22.23 ± 0.11	22.34 ± 0.16	22.25 ± 0.28	...	24.5 ± 5.5	

TABLE 2—*Continued*

Name	α (J2000.0)	δ (J2000.0)	z_{em}[a]	z_{abs}[b]	Type[c]	$\mathcal{R}$[d] (mag)	$G-\mathcal{R}$ (mag)	U_n-G[e] (mag)	J[f] (mag)	K_s[f] (mag)	$m_{3.6\,\mu m}$ (mag)	$m_{4.5\,\mu m}$ (mag)	$m_{5.8\,\mu m}$ (mag)	$m_{8.0\,\mu m}$ (mag)	$f_{24\,\mu m}$ (μJy)	Notes[g]
BM1048	12 36 11.63	62 13 18.3	1.381	1.379	GAL	23.50	0.23	0.23	...	...	22.10 ± 0.07	22.22 ± 0.07	22.47 ± 0.12	22.65 ± 0.18	21.7 ± 4.9	
BM1053	12 36 18.48	62 12 45.9	1.460	1.457	GAL	24.99	0.09	−0.02	...	...	24.02 ± 0.10	24.32 ± 0.20	...	...	15.7 ± 4.3	
BM1061	12 36 15.82	62 13 26.0	2.089	...	GAL	25.37	0.02	−0.05	...	...	23.77 ± 0.15	23.96 ± 0.20	...	...	...	
BM1063	12 36 21.37	62 12 52.9	...	2.087	GAL	24.46	0.20	0.39	23.14	22.84	22.53 ± 0.08	22.54 ± 0.09	22.46 ± 0.34	...	36.9 ± 6.3	
BM1064	12 36 32.06	62 11 40.0	...	1.524	GAL	23.57	0.18	0.28	22.54	22.55	22.48 ± 0.07	22.57 ± 0.08	23.00 ± 0.30	...	25.2 ± 8.2	
BM1069	12 36 11.63	62 14 16.5	...	2.028	GAL	24.43	0.27	0.36	...	...	21.72 ± 0.07	21.67 ± 0.08	21.56 ± 0.18	22.05 ± 0.27	91.1 ± 9.8	
BM1072	12 36 04.15	62 15 21.0	1.143	...	GAL	23.48	0.10	0.29	...	...	22.36 ± 0.07	22.69 ± 0.09	23.32 ± 0.32	...	...	
BM1074	12 36 28.77	62 12 39.4	0.880	...	GAL	24.32	0.11	0.00	23.63	23.42	23.33 ± 0.07	23.99 ± 0.16	23.26 ± 0.24	...	72.0 ± 9.7	
BM1083	12 36 06.67	62 15 50.7	2.414	...	QSO	23.34	0.25	0.26	...	...	21.59 ± 0.07	21.34 ± 0.07	20.73 ± 0.08	20.47 ± 0.07	112.9 ± 11.0	B03-77
BM1092	12 36 13.42	62 15 17.7	1.479	...	GAL	24.07	0.12	0.31	...	...	22.84 ± 0.07	22.86 ± 0.07	23.03 ± 0.20	23.54 ± 0.24	...	
BM1095	12 36 24.64	62 14 18.6	1.450	1.445	GAL	24.31	−0.01	0.15	23.17	23.66	23.37 ± 0.08	23.67 ± 0.15	...	...	...	
BM1098	12 36 51.16	62 11 28.0	...	1.671	GAL	23.76	0.20	0.37	22.77	22.47	22.09 ± 0.07	22.01 ± 0.07	22.45 ± 0.19	22.63 ± 0.19	30.2 ± 5.7	
BM1099	12 37 03.45	62 10 09.1	...	:1.662	GAL	24.67	0.23	0.35	23.73	23.16	23.08 ± 0.11	23.15 ± 0.17	...	...	21.1 ± 4.9	
BM1119.....	12 37 03.70	62 11 22.6	...	1.717	GAL	23.29	0.28	0.32	22.30	21.74	21.60 ± 0.07	21.50 ± 0.07	21.32 ± 0.08	21.56 ± 0.23	152.6 ± 12.4	B03-327
BM1121	12 36 58.38	62 12 13.9	1.020	1.020	GAL	23.11	0.26	0.22	22.52	22.15	22.46 ± 0.20	...	...	...	21.5 ± 5.3	
BM1122	12 37 02.62	62 11 56.7	1.994	1.986	GAL	23.96	0.17	0.33	24.18	24.00	23.27 ± 0.10	23.30 ± 0.16	...	...	...	
BM1132	12 36 53.07	62 13 44.3	...	:1.901	GAL	23.76	0.26	0.40	23.13	22.63	22.98 ± 0.07	23.06 ± 0.07	23.08 ± 0.23	23.27 ± 0.21	...	
BM1135	12 36 49.76	62 14 14.9	...	1.872	GAL	23.57	0.29	0.43	22.44	21.76	21.63 ± 0.07	21.57 ± 0.09	21.49 ± 0.16	21.96 ± 0.30	111.4 ± 10.7	
BM1136	12 36 52.75	62 13 54.8	1.355	...	GAL	22.15	0.16	0.23	21.53	21.36	21.15 ± 0.07	21.11 ± 0.07	21.37 ± 0.20	21.16 ± 0.12	99.5 ± 10.2	B03-272
BM1139	12 37 22.12	62 10 46.6	1.919	...	GAL	24.10	0.25	0.18	24.37	23.17	22.46 ± 0.14	22.61 ± 0.20	...	...	220.8 ± 15.0	
BM1144	12 36 43.72	62 15 46.2	...	:1.660	GAL	25.09	0.22	0.40	23.47	22.92	22.73 ± 0.08	22.70 ± 0.08	22.91 ± 0.29	...	...	
BM1146	12 37 10.65	62 12 56.2	...	:1.926	GAL	24.30	0.09	0.06	23.88	23.29	23.20 ± 0.11	23.55 ± 0.20	...	...	...	
BM1148	12 36 46.15	62 15 51.1	2.053	2.045	GAL	23.38	0.20	0.29	24.43	23.08	23.11 ± 0.07	23.24 ± 0.11	...	23.08 ± 0.30	14.5 ± 4.1	
BM1149	12 36 34.79	62 17 10.1	1.631	1.629	GAL	24.58	0.02	0.16	>25.0	>24.4	24.15 ± 0.25	...	...	...	...	
BM1153	12 36 48.46	62 15 59.5	2.450	2.439	GAL	24.64	0.32	0.47	23.83	22.85	21.65 ± 0.07	21.43 ± 0.07	21.42 ± 0.10	21.54 ± 0.12	123.0 ± 11.2	
BM1155	12 37 23.98	62 12 12.1	2.024	2.015	GAL	23.99	0.08	0.15	23.25	23.50	23.21 ± 0.07	23.28 ± 0.13	...	...	...	
BM1156	12 37 04.34	62 14 46.3	2.211	...	AGN	24.62	−0.01	−0.21	22.94	22.15	22.10 ± 0.07	21.94 ± 0.07	21.18 ± 0.08	19.97 ± 0.07	324.4 ± 18.1	S03-oMD49
BM1158	12 37 18.58	62 13 15.0	...	1.521	GAL	23.35	0.28	0.48	22.19	21.94	21.75 ± 0.07	21.72 ± 0.07	21.96 ± 0.25	21.67 ± 0.07	64.8 ± 8.3	
BM1159	12 37 13.32	62 13 56.4	...	1.016	GAL	22.87	0.10	0.08	22.13	22.03	21.97 ± 0.07	22.41 ± 0.07	22.79 ± 0.15	22.62 ± 0.10	22.1 ± 5.7	
BM1160	12 36 55.63	62 16 01.9	1.364	...	GAL	24.36	0.28	0.36	23.43	23.41	22.93 ± 0.09	23.01 ± 0.12	23.70 ± 0.26	...	19.8 ± 5.1	
BM1161	12 37 08.76	62 14 31.5	2.045	...	GAL	24.94	0.15	0.04	>25.0	23.68	23.97 ± 0.36	...	...	...	...	
BM1163	12 37 26.98	62 12 24.5	1.876	1.872	GAL	24.72	0.23	0.43	23.80	23.56	23.18 ± 0.10	...	22.74 ± 0.36	...	...	
BM1171	12 36 40.34	62 18 53.8	...	2.082	GAL	24.71	0.28	0.36	...	...	23.45 ± 0.17	23.69 ± 0.23	...	...	...	
BM1172	12 37 02.84	62 16 20.5	1.866	1.862	GAL	24.23	0.13	0.15	23.55	23.49	23.60 ± 0.16	23.53 ± 0.17	...	...	...	
BM1174	12 36 56.40	62 17 09.8	...	:1.670	GAL	24.97	0.11	0.14	>25.0	>24.4	22.70 ± 0.07	22.95 ± 0.09	23.38 ± 0.17	23.38 ± 0.30	...	
BM1175	12 37 26.35	62 13 38.5	1.778	1.767	GAL	23.94	0.25	0.30	23.28	23.02	22.53 ± 0.16	22.55 ± 0.20	...	...	14.6 ± 4.6	
BM1180	12 37 27.22	62 13 52.9	...	1.598	GAL	23.55	0.20	0.28	22.21	21.84	22.02 ± 0.12	21.95 ± 0.15	21.97 ± 0.32	...	...	
BM1181	12 37 01.75	62 16 53.0	1.747	1.740	GAL	22.56	0.25	0.35	22.03	22.26	22.47 ± 0.07	22.51 ± 0.07	22.87 ± 0.17	23.31 ± 0.26	15.4 ± 4.0	
BM1190	12 37 06.87	62 17 02.1	1.020	...	QSO	19.81	0.15	−0.02	19.37	19.06	18.63 ± 0.07	18.37 ± 0.07	18.10 ± 0.07	17.79 ± 0.07	866.4 ± 29.5	B03-344
BM1193	12 37 19.33	62 15 59.1	...	:1.564	GAL	24.36	0.20	0.17	22.93	23.30	...	...	...	...	...	
BM1195	12 37 35.59	62 14 05.9	...	1.289	GAL	23.97	0.28	0.37	...	...	21.84 ± 0.07	21.82 ± 0.07	21.99 ± 0.21	...	50.4 ± 7.3	
BM1196	12 37 18.75	62 16 15.0	1.863	...	...	24.62	−0.07	0.00	>25.0	>24.4	24.12 ± 0.22	24.22 ± 0.32	...	...	...	
BM1197	12 37 19.39	62 16 21.0	...	1.566	GAL	23.76	0.20	0.34	22.61	22.38	22.32 ± 0.07	22.28 ± 0.07	22.77 ± 0.21	22.90 ± 0.34	18.8 ± 4.8	
BM1198	12 37 24.06	62 16 05.8	...	1.780	GAL	23.65	0.24	0.43	23.21	22.73	22.38 ± 0.07	22.34 ± 0.09	22.41 ± 0.24	23.05 ± 0.34	39.5 ± 6.5	
BM1200	12 37 30.85	62 15 29.6	...	2.078	GAL	23.79	0.26	0.41	23.86	22.45	22.85 ± 0.10	22.89 ± 0.16	22.99 ± 0.35	...	16.7 ± 5.6	DRG
BM1201	12 37 21.09	62 16 41.9	1.001	...	GAL	24.24	0.09	0.00	23.12	23.26	23.54 ± 0.09	24.00 ± 0.21	...	...	...	
BM1204	12 37 18.29	62 17 09.1	...	1.489	GAL	23.64	0.08	0.19	22.79	22.65	22.53 ± 0.07	22.60 ± 0.10	22.96 ± 0.21	...	22.4 ± 5.2	

TABLE 2—*Continued*

Name	α (J2000.0)	δ (J2000.0)	z_{em}[a]	z_{abs}[b]	Type[c]	$\mathcal{R}$[d] (mag)	$G-\mathcal{R}$ (mag)	U_n-G[e] (mag)	J[f] (mag)	K_s[f] (mag)	$m_{3.6\,\mu m}$ (mag)	$m_{4.5\,\mu m}$ (mag)	$m_{5.8\,\mu m}$ (mag)	$m_{8.0\,\mu m}$ (mag)	$f_{24\,\mu m}$ (μJy)	Notes[g]
BM1205	12 37 42.45	62 14 19.5	1.711	1.711	GAL	24.44	0.11	−0.05	...	...	22.70 ± 0.07	22.54 ± 0.07	22.58 ± 0.13	22.58 ± 0.17	9.4 ± 2.2	
BM1207	12 37 16.19	62 17 30.3	1.083	...	GAL	23.95	0.23	0.26	23.19	23.18	22.47 ± 0.08	23.63 ± 0.20	...	...	171.3 ± 13.3	
BM1209	12 37 30.87	62 15 55.1	...	1.775	GAL	23.44	0.29	0.40	>25.0	22.46	22.28 ± 0.11	22.49 ± 0.15	22.34 ± 0.29	...	15.5 ± 4.9	DRG
BM1211	12 37 43.19	62 14 49.6	0.960	...	GAL	24.47	0.21	0.15	...	...	23.53 ± 0.07	23.84 ± 0.15	...	...	...	
BM1212	12 37 24.28	62 17 20.8	...	:1.379	GAL	23.65	0.10	0.26	22.83	23.36	22.77 ± 0.09	22.74 ± 0.09	...	...	18.4 ± 4.8	
BM1226	12 37 11.63	62 19 58.2	1.355	...	GAL	24.32	0.28	0.39	...	...	23.12 ± 0.07	23.15 ± 0.07	...	...	...	
BM1289	12 37 00.02	62 07 46.2	2.380	...	GAL	24.34	0.45	0.59	...	...	24.13 ± 0.28	24.38 ± 0.35	...	...	20.2 ± 5.0	
BM1293	12 36 58.59	62 08 28.2	:2.300	...	GAL	24.91	0.50	0.66	...	...	22.51 ± 0.12	23.01 ± 0.14	...	...	18.3 ± 4.7	
BM1299	12 37 01.33	62 08 44.6	...	1.595	GAL	23.31	0.44	0.51	...	...	20.91 ± 0.07	21.04 ± 0.07	21.10 ± 0.07	21.27 ± 0.10	...	
BM1303	12 36 39.51	62 11 40.4	...	1.721	GAL	24.75	0.46	0.45	23.56	22.43	22.23 ± 0.08	22.03 ± 0.09	22.06 ± 0.23	22.35 ± 0.26	134.7 ± 11.8	
BM1324	12 36 16.00	62 15 58.2	0.322	0.322	GAL	22.80	0.36	0.52	...	...	22.45 ± 0.07	22.66 ± 0.07	22.50 ± 0.14	...	12.7 ± 3.7	
BM1326	12 36 53.46	62 11 40.0	...	1.268	GAL	22.31	0.28	0.19	21.46	20.47	20.38 ± 0.07	20.29 ± 0.07	20.48 ± 0.07	20.02 ± 0.07	303.2 ± 17.6	B03-277
BM1334	12 37 12.15	62 10 29.6	...	1.893	GAL	23.74	0.43	0.58	22.47	21.96	21.97 ± 0.07	21.89 ± 0.09	22.10 ± 0.26	22.36 ± 0.30	15.3 ± 4.0	
BM1335	12 37 07.82	62 10 57.6	...	1.489	GAL	23.16	0.51	0.55	22.02	21.47	21.15 ± 0.07	21.05 ± 0.07	21.19 ± 0.17	...	...	
BM1339	12 37 09.12	62 11 28.5	...	1.338	GAL	23.17	0.36	0.31	22.40	22.00	21.93 ± 0.07	22.01 ± 0.10	22.37 ± 0.27	22.56 ± 0.33	38.0 ± 6.2	
BM1345	12 37 17.39	62 10 46.7	0.202	...	GAL	22.54	0.37	0.53	21.57	20.87	21.72 ± 0.07	21.96 ± 0.07	21.89 ± 0.07	22.15 ± 0.09	...	
BM1358	12 37 01.24	62 15 20.5	...	1.807	GAL	24.07	0.46	0.64	22.33	21.17	21.11 ± 0.07	20.97 ± 0.07	20.91 ± 0.07	21.22 ± 0.08	202.8 ± 14.4	
BM1362	12 37 07.09	62 14 56.0	...	:1.711	GAL	23.24	0.48	0.64	22.32	21.87	22.10 ± 0.07	22.07 ± 0.07	22.21 ± 0.13	22.74 ± 0.22	33.9 ± 6.2	
BM1369	12 37 07.79	62 15 25.0	...	1.879	GAL	24.56	0.43	0.61	>25.0	23.21	23.59 ± 0.12	23.83 ± 0.20	...	...	167.9 ± 14.3	DRG
BM1375	12 36 58.58	62 17 15.3	2.113	2.106	GAL	23.91	0.30	0.31	22.92	22.75	21.88 ± 0.12	22.09 ± 0.10	22.29 ± 0.23	22.23 ± 0.28	...	
BM1376	12 37 13.85	62 15 38.3	...	:1.278	GAL	23.35	0.46	0.40	22.30	22.12	23.69 ± 0.25	...	...	...	...	
BM1384	12 37 23.15	62 15 38.0	2.243	...	AGN	23.98	0.49	0.45	22.79	21.69	21.91 ± 0.07	21.63 ± 0.07	21.27 ± 0.09	20.75 ± 0.07	63.8 ± 8.2	B03-409
BM1396	12 37 38.38	62 15 09.0	1.743	1.743	GAL	23.66	0.45	0.52	...	...	21.48 ± 0.07	21.39 ± 0.07	21.54 ± 0.07	21.81 ± 0.11	69.2 ± 8.8	
BM1413	12 37 41.39	62 16 45.9	...	:1.391	GAL	22.93	0.42	0.35	...	...	22.39 ± 0.07	22.73 ± 0.10	22.62 ± 0.14	...	...	
BM35	12 37 00.80	62 11 34.0	...	1.875	GAL	23.49	0.43	0.17	22.70	22.68	22.66 ± 0.08	22.96 ± 0.13	...	...	...	
BM63	12 37 13.75	62 14 09.0	:1.912	...	GAL	24.48	0.30	0.21	23.87	>24.4	23.55 ± 0.11	23.56 ± 0.14	...	...	...	
BM69	12 37 17.68	62 14 35.9	:1.991	:1.991	GAL	25.12	0.31	0.27	>25.0	>24.4	...	...	...	...	32.7 ± 5.8	
BM70	12 37 20.05	62 14 57.1	1.997	1.994	GAL	24.05	0.37	0.15	23.11	23.33	23.24 ± 0.07	23.69 ± 0.19	...	...	...	
BM72	12 37 22.00	62 15 03.3	...	1.571	GAL	24.72	0.34	0.18	23.27	23.33	22.24 ± 0.16	...	...	...	...	
C2	12 35 59.42	62 11 19.9	...	2.991	GAL	25.24	0.80	>1.46	...	...	23.35 ± 0.13	23.39 ± 0.19	...	...	...	
C11	12 36 47.88	62 10 31.9	...	2.990	GAL	24.59	0.86	>2.05	>25.0	23.46	23.72 ± 0.11	23.86 ± 0.15	23.25 ± 0.24	...	...	S03-M7; DRG
C12	12 36 51.54	62 10 41.7	...	2.975	GAL	24.41	1.14	>1.95	24.2	23.18	22.63 ± 0.08	22.54 ± 0.09	...	...	23.8 ± 5.4	S03-M9
C14	12 36 54.95	62 11 43.8	...	2.973	GAL	25.30	1.07	>1.13	>25.0	23.79	23.19 ± 0.10	23.16 ± 0.11	...	...	...	
C16	12 36 44.07	62 13 11.0	...	2.929	GAL	23.99	1.14	>2.37	23.26	22.25	22.04 ± 0.07	21.93 ± 0.09	21.68 ± 0.17	21.47 ± 0.22	88.8 ± 9.6	S03-M18
C17	12 37 09.73	62 10 16.6	...	3.384	GAL	24.75	1.16	>1.59	>25.0	>24.4	...	...	...	...	...	
C18	12 36 23.89	62 15 48.8	3.230	...	GAL	25.15	0.56	>1.79	23.96	23.36	23.83 ± 0.15	23.92 ± 0.25	...	...	...	
C20	12 36 24.29	62 15 51.7	2.981	...	GAL	25.28	0.93	>1.29	>25.0	>24.4	...	...	...	...	...	
C29	12 36 48.86	62 15 02.6	3.115	3.105	GAL	24.72	0.73	>2.05	>25.0	23.13	23.25 ± 0.07	23.36 ± 0.08	23.61 ± 0.34	23.25 ± 0.17	43.9 ± 7.1	S03-oC38; DRG
C30	12 36 51.87	62 15 15.4	3.334	3.321	GAL	24.32	0.79	>2.39	>25.0	23.56	23.80 ± 0.19	23.81 ± 0.16	...	...	...	S03-C24; DRG
C33	12 36 49.01	62 15 42.5	3.136	3.125	GAL	23.77	0.45	>3.28	23.68	23.65	23.20 ± 0.13	23.28 ± 0.28	23.22 ± 0.36	...	19.0 ± 4.5	S03-D15
C35	12 36 43.09	62 16 36.0	...	3.363	GAL	24.71	0.91	>1.88	>25.0	23.53	23.09 ± 0.12	23.06 ± 0.11	...	...	32.8 ± 6.0	S03-M32; DRG
C40	12 37 06.19	62 15 10.1	3.246	3.239	GAL	24.53	0.85	>2.12	23.95	23.28	23.68 ± 0.15	23.69 ± 0.22	...	...	...	S03-M27
C41	12 37 21.63	62 13 50.4	3.148	...	GAL	25.14	0.29	>2.07	>25.0	23.87	23.08 ± 0.23	...	...	...	...	S03-C18
C42	12 36 51.29	62 18 15.0	...	3.411	GAL	24.46	1.06	>1.98	...	...	23.56 ± 0.25	23.39 ± 0.26	...	...	...	
C48	12 36 51.81	62 19 06.0	...	3.206	GAL	24.89	0.99	>1.62	...	...	23.73 ± 0.20	23.87 ± 0.25	...	...	...	
C53	12 37 23.38	62 16 23.9	3.103	...	GAL	25.04	0.94	>1.52	>25.0	>24.4	24.07 ± 0.22	23.98 ± 0.21	...	...	13.8 ± 4.1	
C54	12 37 05.98	62 19 04.0	3.217	...	GAL	25.34	0.41	>1.75	...	...	24.44 ± 0.08	24.61 ± 0.18	...	...	...	

TABLE 2—*Continued*

Name	α (J2000.0)	δ (J2000.0)	z_{em}[a]	z_{abs}[b]	Type[c]	$\mathcal{R}$[d] (mag)	$G-\mathcal{R}$ (mag)	U_n-G[e] (mag)	J[f] (mag)	K_s[f] (mag)	$m_{3.6\,\mu m}$ (mag)	$m_{4.5\,\mu m}$ (mag)	$m_{5.8\,\mu m}$ (mag)	$m_{8.0\,\mu m}$ (mag)	$f_{24\,\mu m}$ (μJy)	Notes[g]
S03-C5	12 36 23.88	62 09 43.0	...	:2.664	GAL	24.65	0.71	0.89	24.10	23.54	23.11 ± 0.17	23.40 ± 0.30	...	...	29.9 ± 5.9	S03-C5
S03-C7	12 36 37.64	62 10 47.4	...	2.658	GAL	24.36	0.95	1.23	24.41	23.09	24.25 ± 0.17	24.56 ± 0.33	...	...	20.3 ± 5.1	S03-C7
S03-C8	12 36 26.95	62 11 27.0	2.993	2.983	GAL	24.38	0.85	1.81	23.59	23.96	23.41 ± 0.11	23.49 ± 0.25	...	...	13.3 ± 3.8	S03-C8
S03-C17	12 36 51.17	62 13 48.9	:3.163	...	GAL	24.84	0.60	0.92	>25.0	23.91	23.72 ± 0.26	...	...	...	28.4 ± 5.7	S03-C17
S03-C26	12 37 03.26	62 16 35.0	...	3.239	GAL	23.95	1.31	2.85	23.58	22.66	20.86 ± 0.07	21.30 ± 0.07	21.50 ± 0.10	21.61 ± 0.18	43.2 ± 6.8	S03-C26
S03-oC14	12 36 50.36	62 10 55.3	:2.928	...	GAL	25.61	0.36	1.21	...	...	...	...	...	...	53.3 ± 8.6	S03-oC14
S03-oC26	12 36 34.83	62 12 53.6	:3.182	...	GAL	25.63	0.40	1.66	...	...	...	...	...	...	...	S03-oC26
S03-oC29	12 36 45.35	62 13 46.7	:3.161	...	GAL	25.49	0.64	1.59	...	...	...	...	...	...	...	S03-oC29
S03-oC34	12 36 33.49	62 14 17.9	:3.413	...	QSO	25.32	1.05	1.58	24.21	22.92	22.65 ± 0.07	22.42 ± 0.07	22.21 ± 0.15	21.91 ± 0.19	19.3 ± 5.0	S03-oC34; B03-176
D8.....	12 35 59.84	62 12 08.7	3.300	...	GAL	25.10	0.93	2.80	...	...	...	...	...	...	...	
D14.....	12 36 45.02	62 09 40.6	2.983	2.975	GAL	24.97	0.37	1.92	24.69	23.97	...	...	...	...	...	S03-MD10
D16.....	12 36 17.49	62 13 10.1	2.930	...	GAL	25.06	−0.01	1.76	...	...	24.42 ± 0.10	24.79 ± 0.23	...	...	9.7 ± 2.6	S03-D11
D19.....	12 36 41.84	62 11 07.1	3.199	3.187	GAL	24.45	0.68	3.23	24.03	23.33	24.07 ± 0.21	23.94 ± 0.28	...	...	...	S03-MD22
D20.....	12 36 49.46	62 10 18.5	3.247	...	GAL	25.26	0.76	2.74	24.45	23.22	24.43 ± 0.17	24.71 ± 0.22	...	...	13.0 ± 4.1	
D23.....	12 36 19.37	62 15 01.9	3.128	3.123	GAL	23.78	0.62	2.45	23.47	22.96	...	...	...	...	...	S03-C22
D25.....	12 36 46.94	62 12 26.2	2.970	...	GAL	24.25	0.14	1.94	>25.0	>24.4	24.86 ± 0.23	25.13 ± 0.31	...	...	...	S03-D10
D26.....	12 36 14.69	62 16 22.9	2.975	...	GAL	25.48	0.29	1.79	...	...	24.07 ± 0.24	23.97 ± 0.25	...	...	18.5 ± 5.1	
D28.....	12 36 47.79	62 12 55.7	...	2.932	GAL	24.02	0.95	2.55	23.38	22.35	22.36 ± 0.07	22.30 ± 0.08	22.16 ± 0.16	22.06 ± 0.14	40.1 ± 7.1	S03-M17
D29.....	12 37 16.91	62 10 02.1	3.451	...	GAL	24.09	0.82	3.37	24.06	23.66	24.04 ± 0.23	...	...	...	75.0 ± 9.1	S03-C6
D32.....	12 36 42.39	62 14 49.0	2.962	...	GAL	24.87	0.18	2.38	>25.0	>24.4	24.11 ± 0.16	24.17 ± 0.22	...	...	13.0 ± 4.0	S03-D14
D34.....	12 36 37.14	62 15 48.0	2.975	2.970	GAL	25.46	0.62	2.22	>25.0	24.21	23.42 ± 0.10	23.65 ± 0.13	23.62 ± 0.26	...	...	S03-C25
D35.....	12 36 53.62	62 14 10.3	3.196	...	GAL	24.88	1.00	2.76	24.04	23.50	23.72 ± 0.11	23.82 ± 0.17	...	...	8.9 ± 2.9	S03-M22
D38.....	12 36 39.27	62 17 13.1	2.944	2.936	GAL	24.48	0.71	2.35	23.92	23.32	23.07 ± 0.18	23.01 ± 0.24	22.72 ± 0.28	22.69 ± 0.34	...	S03-C27
D39.....	12 37 00.54	62 14 41.9	...	2.987	GAL	24.82	0.61	2.14	24.60	>24.4	24.36 ± 0.26	...	...	...	...	
D41.....	12 36 43.42	62 17 51.8	3.228	...	GAL	24.77	0.84	3.20	24.19	23.46	23.86 ± 0.07	23.84 ± 0.07	...	23.92 ± 0.35	...	
D45.....	12 36 58.98	62 17 14.2	3.134	3.127	GAL	23.58	1.05	3.09	21.86	20.92	20.93 ± 0.07	21.22 ± 0.07	21.43 ± 0.17	21.44 ± 0.18	...	S03-C28
D47.....	12 37 24.37	62 14 31.9	3.193	3.188	GAL	25.16	0.44	3.23	>25.0	>24.4	24.35 ± 0.33	24.21 ± 0.26	...	...	...	
D55.....	12 36 55.29	62 19 47.9	3.251	3.239	GAL	23.92	1.14	2.86	...	...	23.27 ± 0.07	23.22 ± 0.07	23.35 ± 0.26	23.04 ± 0.26	...	
S03-D3	12 36 47.70	62 10 53.2	...	2.943	GAL	24.18	0.81	1.47	23.68	23.60	...	...	...	...	...	S03-D3
S03-D6	12 37 12.27	62 11 37.8	2.925	...	GAL	25.40	0.14	2.00	...	...	...	...	...	...	35.7 ± 6.2	S03-D6
S03-oD3	12 36 48.31	62 09 51.7	:2.729	2.720	GAL	24.52	0.68	0.62	>25.0	24.13	23.86 ± 0.19	...	...	...	15.4 ± 4.5	S03-oD3
S03-oD12	12 36 20.51	62 14 17.8	:2.418	...	GAL	24.59	0.58	0.74	24.18	23.67	23.16 ± 0.15	23.10 ± 0.22	...	...	96.5 ± 10.0	S03-oD12
MD4	12 35 56.54	62 11 26.1	2.867	...	GAL	25.22	0.38	1.55	...	...	23.97 ± 0.23	...	...	...	...	
MD6	12 36 02.68	62 10 59.8	3.246	3.241	GAL	24.38	0.87	2.00	...	...	22.70 ± 0.07	22.57 ± 0.21	...	22.68 ± 0.32	114.6 ± 10.8	
MD13	12 35 59.63	62 12 00.6	...	2.974	GAL	24.01	0.91	2.31	...	...	22.37 ± 0.08	22.57 ± 0.16	...	...	...	
MD27	12 36 42.96	62 09 58.1	3.661	...	GAL	25.48	1.00	2.46	22.86	21.04	20.59 ± 0.07	20.50 ± 0.07	20.33 ± 0.07	20.76 ± 0.08	21.0 ± 4.8	DRG
MD31	12 36 22.58	62 13 06.5	2.981	...	GAL	24.92	0.53	1.69	24.57	23.13	22.03 ± 0.07	21.95 ± 0.11	21.70 ± 0.20	21.83 ± 0.32	13.4 ± 4.1	S03-C14; B03-133; DRG
MD33	12 36 25.56	62 13 50.5	...	2.932	GAL	24.40	0.68	1.88	23.42	23.38	22.94 ± 0.10	23.03 ± 0.07	22.94 ± 0.17	23.42 ± 0.21	...	
MD34	12 36 41.25	62 12 03.1	3.222	3.214	GAL	24.26	0.91	2.39	24.17	22.78	23.79 ± 0.08	23.78 ± 0.11	23.97 ± 0.30	...	97.3 ± 9.9	S03-C11; DRG
MD39	12 36 22.94	62 15 26.7	2.583	...	QSO	20.48	−0.23	0.78	20.19	20.07	20.04 ± 0.07	19.98 ± 0.07	19.45 ± 0.07	18.82 ± 0.07	487.9 ± 22.2	B03-137
MD43	12 36 40.87	62 13 58.5	...	3.087	GAL	24.04	0.66	2.02	23.01	22.42	22.25 ± 0.07	22.48 ± 0.07	22.55 ± 0.24	22.95 ± 0.31	38.6 ± 6.5	S03-D13
MD48	12 37 06.64	62 14 00.2	...	2.926	GAL	24.89	0.69	1.79	24.01	23.36	22.74 ± 0.07	22.62 ± 0.07	22.67 ± 0.15	22.46 ± 0.20	34.5 ± 6.6	S03-M21
MD49	12 37 25.45	62 12 00.9	...	2.850	GAL	23.95	0.62	1.75	24.01	22.96	23.13 ± 0.09	23.15 ± 0.14	23.13 ± 0.28	23.05 ± 0.27	15.6 ± 4.2	
MD50	12 36 51.43	62 16 08.3	3.238	3.234	GAL	24.77	0.99	2.04	>25.0	>24.4	24.09 ± 0.15	24.04 ± 0.13	...	...	...	
MD54	12 37 32.35	62 13 11.2	2.939	...	GAL	25.10	0.54	1.99	...	...	23.15 ± 0.17	23.03 ± 0.19	...	...	...	
MD55	12 37 16.11	62 15 26.5	...	2.956	GAL	24.86	0.69	2.13	>25.0	>24.4	23.54 ± 0.11	23.52 ± 0.21	...	...	12.8 ± 3.8	
MD74	12 37 01.27	62 21 32.6	2.635	...	GAL	24.45	0.45	1.58	...	...	21.99 ± 0.07	21.73 ± 0.07	21.34 ± 0.12	20.78 ± 0.07	123.4 ± 11.3	

TABLE 2—*Continued*

Name	α (J2000.0)	δ (J2000.0)	z_{em}[a]	z_{abs}[b]	Type[c]	$\mathcal{R}$[d] (mag)	$G-\mathcal{R}$ (mag)	U_n-G[e] (mag)	J[f] (mag)	K_s[f] (mag)	$m_{3.6\,\mu m}$ (mag)	$m_{4.5\,\mu m}$ (mag)	$m_{5.8\,\mu m}$ (mag)	$m_{8.0\,\mu m}$ (mag)	$f_{24\,\mu m}$ (μJy)	Notes[g]
MD75	12 37 37.09	62 17 04.6	...	2.790	GAL	24.03	1.08	2.30	...	...	22.19 ± 0.07	22.63 ± 0.12	22.70 ± 0.15	22.73 ± 0.35	25.4 ± 5.8	
MD78	12 37 07.72	62 21 00.3	2.812	...	GAL	24.83	0.27	1.51	...	...	...	...	...	...	...	
MD79	12 37 10.91	62 20 44.7	...	:2.291	GAL	24.44	0.35	1.58	...	...	22.92 ± 0.09	22.82 ± 0.10	22.62 ± 0.16	23.01 ± 0.35	23.2 ± 5.1	
MD83	12 37 21.57	62 20 11.0	...	3.213	GAL	24.35	0.62	1.77	...	...	23.95 ± 0.21	24.26 ± 0.31	...	...	9.7 ± 3.0	
S03-MD3	12 36 33.05	62 09 03.3	:2.898	...	GAL	23.94	0.87	1.48	...	...	20.65 ± 0.07	21.13 ± 0.07	21.46 ± 0.23	22.00 ± 0.29	22.4 ± 5.0	S03-MD3
S03-MD12	12 37 19.86	62 09 54.9	:2.647	...	AGN	24.36	0.72	0.92	23.41	22.11	21.59 ± 0.07	21.20 ± 0.07	20.48 ± 0.07	19.85 ± 0.07	139.7 ± 12.0	S03-MD12; B03-398
S03-MD45	12 37 14.18	62 16 28.6	:2.345	...	GAL	23.63	0.57	0.82	22.00	21.50	21.07 ± 0.07	20.91 ± 0.07	20.97 ± 0.07	21.23 ± 0.10	178.1 ± 13.5	S03-MD45
S03-oMD19	12 36 37.00	62 10 43.8	...	3.241	GAL	24.04	0.68	1.48	23.75	22.72	23.31 ± 0.07	23.25 ± 0.07	23.23 ± 0.24	22.90 ± 0.20	18.5 ± 4.9	S03-oMD19
S03-oMD56	12 36 38.40	62 15 39.5	:0.000	0.000	STAR	23.24	0.82	1.45	23.40	23.75	23.73 ± 0.13	24.13 ± 0.23	23.79 ± 0.26	...	...	S03-oMD56
S03-M16	12 37 17.38	62 12 46.8	...	2.939	GAL	24.67	0.52	1.02	23.99	23.78	23.49 ± 0.11	23.52 ± 0.15	...	...	32.0 ± 6.4	S03-M16
S03-M23	12 37 02.68	62 14 25.9	...	3.214	GAL	24.61	1.09	2.43	...	...	20.83 ± 0.07	20.88 ± 0.07	21.04 ± 0.07	21.08 ± 0.07	...	S03-M23
S03-M25	12 36 50.80	62 14 44.5	...	3.106	GAL	24.70	0.82	1.69	>25.0	23.85	24.32 ± 0.33	...	...	...	...	S03-M25
S03-M35	12 36 45.18	62 16 52.1	...	3.229	GAL	24.05	1.24	3.12	23.34	22.57	22.76 ± 0.08	22.65 ± 0.09	22.35 ± 0.14	22.47 ± 0.20	23.5 ± 5.2	S03-M35

NOTE.—Units of right ascension are hours, minutes, and seconds, and units of declination are degrees, arcminutes, and arcseconds.

[a] Emission-line redshift. An entry with a colon indicates that the redshift is uncertain. A blank entry indicates that an emission-line redshift could not be measured.

[b] Absorption-line redshift. An entry with a colon indicates that the redshift is uncertain. A blank entry indicates that an absorption-line redshift could not be measured.

[c] Source type, either galaxy ("GAL"), "AGN," "QSO," or "STAR." The distinction between QSO and AGN classification is based on the line widths, as described in Steidel et al. (2002), where an object is classified as a "QSO" if it has any emission line with FWHM > 2000 km s^{-1}. AGNs identified using other means (X-ray or mid-IR emission) are discussed in § 6.2.

[d] $\mathcal{R}$ magnitude in AB units.

[e] Upper limits given for galaxies undetected in U_n.

[f] A blank entry indicates that the object did not lie in the region with near-IR imaging.

[g] Galaxies in common with the LBG survey in the HDF-N are indicated by their names ("S03-XXX") as given in Steidel et al. (2003). Galaxies with X-ray counterparts within 1.″5 are indicated by their names ("B03-XXX") in the spectroscopic follow-up to the *Chandra* 2 Ms survey by Barger et al. (2003). Galaxies satisfying the distant red galaxy (DRG) criteria of Franx et al. (2003) are indicated by "DRG."

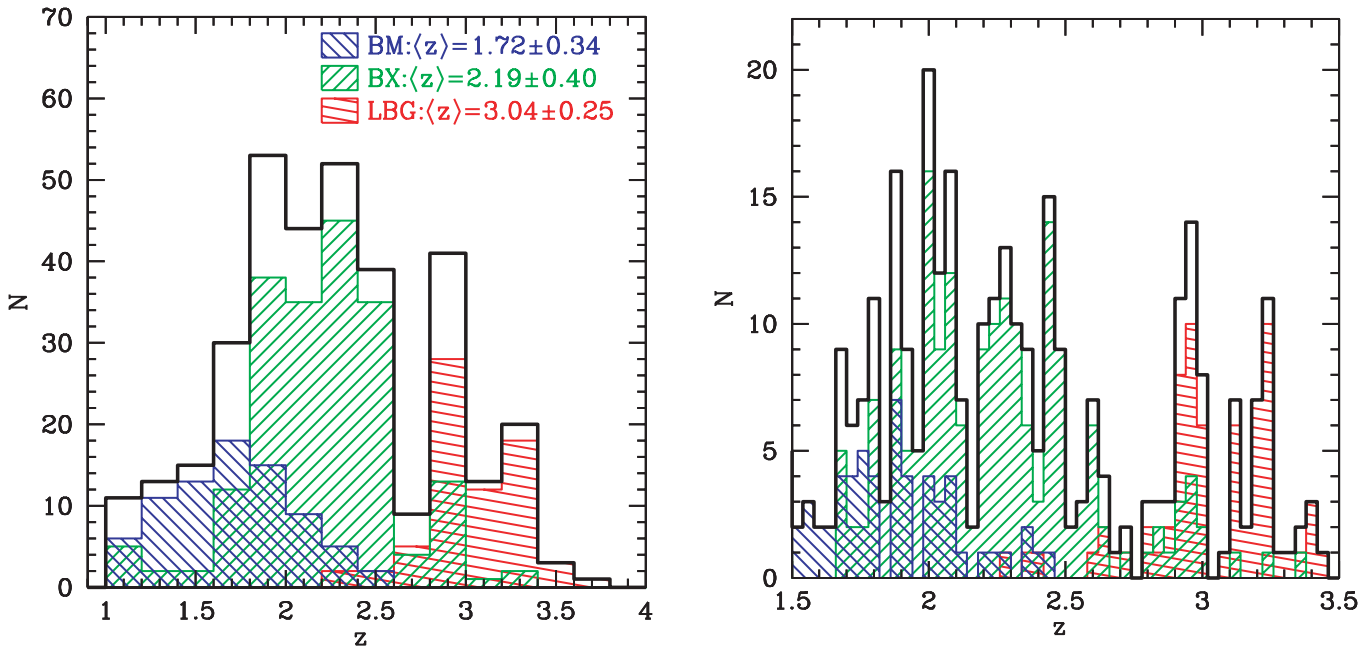

FIG. 3.—*Left*: Redshift histogram of spectroscopically confirmed BM/BX and LBG galaxies in the GOODS-N field with $z > 1$. The solid line indicates the total distribution of BM, BX, and LBG galaxies. *Right*: Redshift histogram with higher resolution bins, $\delta z = 0.04$, emphasizing large-scale structure in GOODS-N.

not accounted for the selection function and relative fractions of candidates observed. Therefore, the significance of any redshift "overdensities" appearing in Figure 3 is not quantified.

4. *SPITZER* IRAC AND MIPS DATA

To aid in understanding the stellar populations and extinction of $z \sim 2$ galaxies, we compiled *Spitzer* IRAC and MIPS photometry for our sample of $U_nG\mathcal{R}$-selected galaxies using the public *Spitzer* data in the GOODS-N field (M. Dickinson et al. 2006, in preparation; R. Chary et al. 2006, in preparation). The IRAC photometry was performed by fitting an empirical point-spread function (PSF) determined from the IRAC images to the spatial positions of sources from the higher resolution K_s band data. Specifically, to accurately compute the empirical PSF for each IRAC channel, we used as many isolated point sources located throughout the IRAC images as possible. Changing the number of objects used to compute the PSF results in variations of the best-fit fluxes of <5% and is generally small compared to the background noise (see below). Using the K_s band data to constrain source positions mitigates the effects of confusion by allowing for the deblending of partially resolved sources in the IRAC images and is similar to the method employed by the GOODS team for extracting photometry (M. Dickinson et al. 2006, in preparation; R. Chary et al. 2006, in preparation; see also Labbé et al. 2005; Shapley et al. 2005). We extracted the MIPS 24 μm fluxes of $U_nG\mathcal{R}$ galaxies using a similar procedure; the spatial positions of sources from the IRAC data were used to deblend and extract the 24 μm fluxes (Reddy et al. 2006). Errors for both IRAC and MIPS photometry were computed from the dispersion of extracted fluxes for 100 PSFs fitted to random blank regions around each galaxy. Since the IRAC and MIPS data are background limited, the errors will be dominated by the background noise for all but the brightest galaxies at these wavelengths. The IRAC channel 1–4 magnitudes and MIPS 24 μm fluxes are listed in Table 2. We do not give fluxes for those galaxies that were either undetected or badly blended with a nearby bright source. Of the 212 BX/BM galaxies with secure spectroscopic redshifts $z > 1.4$, only 2 (<1%) are undetected at 3.6 μm to the GOODS IRAC depth. Of the 74 LBGs, 11 (≈15%) are undetected at 3.6 μm. The MIPS detection fraction is ≈65% for BX/BM galaxies, decreasing to ≈53% for the LBGs, to a limiting 3 σ flux of $f_{24\ \mu\mathrm{m}} \approx 8$ μJy.

5. STELLAR POPULATION MODELING

The combination of multiwavelength photometry and spectroscopic redshifts allows us to better constrain the stellar populations of UV-selected galaxies than if we only had photometric redshifts. To demonstrate the wide range in stellar populations of UV-selected galaxies at redshifts $z \sim 2$–3, we fitted the $U_nG\mathcal{R}JK_s$+IRAC magnitudes with Bruzual & Charlot (2003) models assuming a Salpeter (1955) initial mass function (IMF) and solar metallicity. The assumption of solar metallicity is a reasonable approximation for most galaxies in the $U_nG\mathcal{R}$-selected sample (Erb et al. 2006a). The models were corrected for the effects of IGM opacity before comparing to the observed magnitudes. In fitting the stellar populations, we assumed an exponentially declining star formation history with decay timescales $\tau = 10$, 20, 50, 100, 200, 500, 1000, 2000, and 5000 Myr, and $\tau = \infty$ (constant star formation [CSF] model). We also assumed a varying amount of reddening, or $E(B-V)$, from 0.0 to 0.7. The best-fit model was taken to be the combination of τ, age, and $E(B-V)$ that gave the lowest χ^2 value with respect to the observed magnitudes. The star formation rate (SFR) and stellar mass are determined from the normalization of the model to the observed magnitudes. Even with spectroscopic redshifts, there is considerable uncertainty in the best-fit parameters, with the exception of the total stellar mass M^*, which is generally robust to changes in the assumed star formation history (e.g., Papovich et al. 2001; Shapley et al. 2001, 2005; Sawicki & Yee 1998; Erb et al. 2006c). The best-fit stellar population parameters for both a CSF and τ model for each galaxy are collected in Table 3. Monte Carlo simulations indicate that the typical fractional uncertainties associated

TABLE 3

STELLAR POPULATION PARAMETERS

Name[a]	z	$E(B-V)_\infty$	Age_∞ (Myr)	SFR_∞ ($M_\odot$ yr^{-1})	M^*_∞ ($10^{10}\,M_\odot$)	τ[b] (Myr)	$E(B-V)_\tau$	Age_τ (Myr)	SFR_τ ($M_\odot$ yr^{-1})	M^*_τ ($10^{10}\,M_\odot$)	Notes[c]
BX1035.....	2.236	0.24	20	234	0.466	20	0.24	15	185	0.419	
BX1040.....	2.468	0.09	2100	14	3.030	200	0.03	571	7	2.220	
BX1042.....	2.607	0.18	509	36	1.820	200	0.15	321	23	1.810	
BX1050.....	2.322	0.27	15	118	0.179	50	0.26	15	98	0.173	
BX1051.....	2.098	0.12	404	24	0.963	100	0.02	286	7	1.100	
BX1055.....	2.491	0.12	255	37	0.956	100	0.04	227	14	1.210	
BX1060.....	2.081	0.24	806	64	5.150	100	0.01	509	4	5.810	
BX1064.....	2.086	0.14	509	22	1.100	100	0.02	321	5	1.230	
BX1065.....	2.701	0.08	1434	35	5.040	100	0.00	360	10	3.570	
BX1071.....	1.996	0.21	161	43	0.690	10	0.14	55	2	0.600	
BX1074.....	1.750	0.20	1139	26	2.970	100	0.09	360	7	2.490	
BX1075.....	2.221	0.25	128	91	1.160	50	0.09	203	8	2.270	
BX1080.....	2.390	0.25	203	78	1.590	50	0.11	203	9	2.430	
BX1081.....	1.801	0.24	286	46	1.310	50	0.06	255	2	2.030	
BX1084.....	2.437	0.12	227	82	1.860	100	0.05	227	29	2.570	
BX1085.....	2.236	0.30	10	201	0.201	20	0.08	90	3	0.602	
BX1086.....	2.444	0.28	20	139	0.277	50	0.06	203	4	1.250	
BX1089.....	2.049	0.17	1609	33	5.360	100	0.06	404	7	4.160	
BX1100.....	2.079	0.14	255	68	1.720	50	0.10	114	34	1.510	
BX1104.....	2.441	0.11	286	37	1.050	100	0.05	227	15	1.280	
BX1106.....	2.917	0.10	905	29	2.670	100	0.01	321	9	2.160	
BX1116.....	2.048	0.13	571	29	1.650	100	0.00	360	5	1.900	
BX1121.....	1.878	0.17	806	45	3.640	100	0.02	404	7	3.850	
BX1125.....	2.222	0.15	203	15	0.304	50	0.01	203	2	0.456	
BX1129.....	1.973	0.17	203	122	2.480	50	0.10	143	37	3.110	
BX1140.....	1.487	0.18	806	13	1.070	100	0.01	454	1	1.240	
BX1145.....	2.325	0.07	806	7	0.562	200	0.02	454	3	0.571	
BX1157.....	2.081	0.08	3000	22	6.720	500	0.02	1278	10	5.740	
BX1161.....	1.891	0.24	203	86	1.740	20	0.17	90	11	1.930	
BX1164.....	2.593	0.15	15	67	0.101	∞	0.15	15	67	0.101	
BX1166.....	1.334	0.14	1139	6	0.649	100	0.00	404	1	0.544	
BX1169.....	1.871	0.17	454	33	1.490	100	0.07	286	10	1.680	
BX1170.....	2.443	0.20	806	49	3.950	100	0.04	404	7	3.710	
BX1172.....	2.806	0.20	10	127	0.127	50	0.00	161	5	0.571	
BX1174.....	2.349	0.07	719	18	1.300	5000	0.07	719	18	1.360	
BX1185.....	2.205	0.26	719	39	2.820	200	0.21	404	22	2.820	
BX1186.....	2.079	0.22	10	52	0.052	10	0.20	10	26	0.045	
BX1192.....	1.996	0.18	2600	36	9.450	100	0.10	404	11	5.980	
BX1197.....	2.593	0.06	1434	23	3.350	500	0.04	719	19	2.990	
BX1201.....	2.000	0.15	203	33	0.671	20	0.04	102	3	0.797	
BX1204.....	2.205	0.21	640	36	2.330	50	0.05	255	3	2.250	
BX1208.....	2.589	0.20	15	104	0.157	100	0.01	255	7	0.786	
BX1222.....	2.442	0.21	9	102	0.093	10	0.20	8	69	0.090	
BX1228.....	1.997	0.35	8	375	0.312	20	0.34	8	276	0.284	
BX1229.....	1.343	0.26	50	50	0.251	10	0.24	20	25	0.162	
BX1233.....	2.856	0.07	2200	26	5.780	1000	0.00	2100	10	7.240	
BX1238.....	2.261	0.14	640	25	1.590	200	0.09	404	13	1.640	
BX1240.....	2.282	0.14	114	44	0.507	10	0.05	50	3	0.460	
BX1244.....	1.012	0.28	20	50	0.100	20	0.28	15	40	0.090	
BX1245.....	2.093	0.01	1015	15	1.540	500	0.00	571	13	1.390	
BX1250.....	1.855	0.15	640	18	1.150	100	0.07	286	7	1.110	
BX1252.....	2.931	0.07	255	36	0.917	50	0.00	161	9	1.050	
BX1253.....	1.933	0.13	1139	19	2.190	200	0.05	571	7	2.240	
BX1264.....	2.942	0.00	2100	10	2.140	5000	0.00	2100	10	2.640	
BX1265.....	2.434	0.12	255	34	0.873	50	0.01	180	6	1.060	
BX1267.....	1.996	0.11	1900	22	4.100	5000	0.10	2500	25	8.120	IRAC
BX1269.....	2.275	0.24	255	127	3.250	50	0.17	143	41	3.440	
BX1274.....	2.596	0.10	640	32	2.050	∞	0.10	640	32	2.050	
BX1277.....	2.268	0.09	454	25	1.110	100	0.00	286	7	1.200	
BX1281.....	2.410	0.13	509	14	0.694	100	0.00	360	2	0.809	
BX1283.....	2.427	0.10	2600	17	4.340	200	0.00	719	5	3.260	
BX1284.....	2.273	0.07	1139	14	1.540	100	0.00	321	5	1.150	
BX1287.....	1.675	0.28	9	305	0.278	10	0.00	90	0	0.921	
BX1288.....	2.301	0.08	509	21	1.060	100	0.00	286	7	1.110	

TABLE 3—*Continued*

Name[a]	z	$E(B-V)_\infty$	Age_∞ (Myr)	SFR_∞ ($M_\odot$ yr^{-1})	M^*_∞ (10^{10} $M_\odot$)	τ[b] (Myr)	$E(B-V)_\tau$	Age_τ (Myr)	SFR_τ ($M_\odot$ yr^{-1})	M^*_τ (10^{10} $M_\odot$)	Notes[c]
BX1289	2.488	0.17	404	46	1.850	50	0.06	203	7	2.000	
BX1290	2.980	0.00	905	11	1.020	∞	0.00	905	11	1.020	
BX1291	2.052	0.31	7	469	0.339	100	0.31	7	448	0.336	
BX1296	1.988	0.23	3250	56	18.300	5000	0.20	3250	43	19.900	
BX1297	2.274	0.24	2750	37	10.200	200	0.06	806	7	7.550	
BX1303	2.305	0.10	1700	11	1.800	100	0.01	360	3	1.190	
BX1305	2.234	0.15	2100	17	3.480	200	0.01	719	4	2.780	
BX1307	2.002	0.20	404	92	3.720	10	0.18	50	12	1.810	
BX1311	2.484	0.10	286	58	1.660	50	0.00	180	11	1.890	
BX1313	2.635	0.20	15	121	0.183	1000	0.20	15	120	0.183	
BX1315	1.671	0.22	571	46	2.620	100	0.17	255	22	2.560	
BX1316	2.088	0.13	3000	23	6.980	1000	0.10	1434	18	5.670	
BX1317	1.789	0.18	321	46	1.480	20	0.09	102	4	1.410	K_s
BX1324	1.818	0.34	509	65	3.320	10	0.26	90	0	2.710	
BX1326	2.984	0.00	806	13	1.040	∞	0.00	806	13	1.040	
BX1327	2.209	0.07	1139	16	1.870	200	0.01	509	7	1.750	
BX1330	2.363	0.06	571	27	1.520	100	0.01	255	12	1.410	
BX1332	2.214	0.29	15	282	0.427	20	0.09	90	8	1.400	
BX1334	3.371	0.00	1800	9	1.700	500	0.00	1609	9	10.500	
BX1339	1.988	0.09	1139	13	1.450	100	0.01	321	5	1.090	
BX1343	2.268	0.13	1015	31	3.170	100	0.02	360	7	2.650	
BX1348	1.921	0.09	509	9	0.468	100	0.01	255	4	0.426	
BX1349	1.873	0.33	509	87	4.440	∞	0.33	509	87	4.440	
BX1354	2.088	0.03	321	6	0.199	100	0.00	180	4	0.189	
BX1358	2.943	0.04	641	12	0.753	100	0.00	255	6	0.660	
BX1362	1.664	0.14	1609	16	2.580	200	0.10	509	9	2.160	
BX1363	2.297	0.16	719	37	2.630	100	0.00	404	5	2.760	
BX1364	2.183	0.15	719	29	2.110	100	0.06	321	8	1.980	
BX1368	2.443	0.16	454	61	2.790	100	0.07	286	18	3.000	
BX1376	2.430	0.07	255	16	0.416	50	0.00	143	5	0.426	
BX1378	1.971	0.21	203	56	1.130	20	0.14	81	10	1.100	
BX1387	2.324	0.11	640	14	0.929	200	0.07	360	9	0.897	
BX1388	2.032	0.29	3000	43	13.000	500	0.21	1139	24	10.400	
BX1391	1.906	0.22	203	50	1.010	20	0.14	90	6	1.120	
BX1397	2.133	0.15	1015	30	3.080	100	0.04	360	7	2.650	
BX1399	2.033	0.18	1800	15	2.670	200	0.14	509	9	2.050	
BX1401	2.481	0.18	1139	85	9.650	100	0.01	454	9	8.580	
BX1408	2.482	0.28	640	57	3.680	100	0.15	360	11	3.880	
BX1409	2.237	0.29	2000	34	6.740	100	0.14	454	5	4.810	K_s
BX1420	2.133	0.24	255	87	2.210	50	0.12	180	15	2.720	
BX1425	1.864	0.10	905	10	0.903	100	0.00	321	3	0.769	
BX1427	2.548	0.13	719	29	2.070	100	0.01	360	6	2.050	
BX1431	2.001	0.11	321	24	0.770	100	0.02	255	8	0.918	
BX1434	1.994	0.15	454	21	0.956	200	0.13	286	15	0.931	
BX1439	2.188	0.18	2750	34	9.270	200	0.05	719	9	6.590	K_s
BX1443	1.684	0.30	571	135	7.730	∞	0.30	571	135	7.730	
BX1446	2.320	0.12	321	32	1.040	100	0.05	255	11	1.290	
BX1451	2.245	0.21	905	41	3.740	200	0.18	404	25	3.330	
BX1458	1.864	0.28	509	31	1.570	50	0.13	227	3	1.560	
BX1460	3.134	0.00	2000	14	2.870	2000	0.00	1700	12	3.170	
BX1461	2.107	0.15	255	20	0.514	200	0.14	203	15	0.535	
BX1479	2.377	0.10	905	22	1.950	100	0.03	321	7	1.600	
BX1480	2.545	0.21	203	80	1.630	5000	0.21	203	79	1.640	
BX1485	2.548	0.14	1139	105	11.900	∞	0.14	1139	105	11.900	
BX1495	2.247	0.13	1139	13	1.470	100	0.00	404	2	1.210	
BX1501	1.877	0.18	321	50	1.600	100	0.06	321	10	2.350	
BX1504	2.864	0.09	255	29	0.743	50	0.00	161	7	0.827	
BX1514	2.135	0.17	1900	18	3.450	200	0.06	640	6	2.870	K_s
BX1525	1.689	0.29	1609	39	6.310	200	0.24	509	23	5.350	
BX1530	2.421	0.14	360	29	1.030	500	0.14	286	26	1.010	
BX1535	2.299	0.27	15	159	0.241	20	0.09	90	4	0.797	
BX1542	1.018	0.31	15	25	0.038	200	0.31	15	24	0.038	
BX1559	2.408	0.06	719	21	1.480	∞	0.06	719	21	1.480	
BX1567	2.225	0.19	571	73	4.150	50	0.05	227	9	4.030	
BX1568	1.787	0.23	15	145	0.220	10	0.00	102	0	0.997	

TABLE 3—*Continued*

Name[a]	z	$E(B-V)_\infty$	Age_∞ (Myr)	SFR_∞ ($M_\odot$ yr^{-1})	M^*_∞ ($10^{10}\,M_\odot$)	τ[b] (Myr)	$E(B-V)_\tau$	Age_τ (Myr)	SFR_τ ($M_\odot$ yr^{-1})	M^*_τ ($10^{10}\,M_\odot$)	Notes[c]
BX1572.....	1.782	0.34	8	199	0.165	∞	0.34	8	199	0.165	
BX1574.....	1.808	0.26	806	41	3.270	50	0.14	227	6	2.840	
BX1588.....	2.221	0.25	143	207	2.960	10	0.15	64	5	3.220	
BX1605.....	1.974	0.01	571	13	0.723	1000	0.00	454	12	0.689	
BX1616.....	2.205	0.04	2500	5	1.250	500	0.01	905	4	0.967	
BX1617.....	2.320	0.12	321	13	0.419	∞	0.12	404	13	0.516	
BX1630.....	2.220	0.07	456	16	0.727	100	0.01	255	7	0.771	
BX1636.....	2.300	0.28	255	129	3.300	10	0.24	45	20	1.770	
BX1641.....	1.433	0.22	10	54	0.055	50	0.22	10	48	0.053	
BX1642.....	2.007	0.14	360	25	0.914	∞	0.14	360	25	0.914	
BX1650.....	2.097	0.17	203	85	1.730	50	0.07	161	19	2.270	
BX1694.....	2.007	0.12	360	38	1.370	100	0.05	255	14	1.650	
BX1708.....	1.987	0.34	1278	78	9.940	10	0.41	30	84	1.600	
BX1817.....	1.860	0.37	114	109	1.240	50	0.36	72	74	1.180	
BX1820.....	2.457	0.34	360	191	6.870	∞	0.34	360	191	6.870	
BX1821.....	2.590	0.20	286	41	1.180	100	0.10	286	10	1.610	
BX1823.....	1.818	0.40	2750	69	18.900	200	0.26	719	20	14.300	
BX1826.....	2.929	0.01	2100	12	2.540	200	0.00	509	8	1.810	
BX1827.....	1.988	0.46	7	392	0.284	∞	0.46	7	392	0.284	
BX1848.....	2.648	0.07	571	12	0.700	100	0.00	321	3	0.792	
BX82.....	1.023	0.20	404	6	0.225	10	0.01	227	0	0.310	
BX84.....	2.163	0.16	1278	38	4.860	∞	0.16	1278	38	4.860	
BX150.....	2.277	0.16	2400	26	6.290	100	0.06	321	10	2.350	
BX184.....	1.998	0.45	7	676	0.489	∞	0.45	7	676	0.489	
BX305.....	2.482	0.29	719	88	6.300	100	0.17	360	18	6.290	
BX308.....	2.376	0.21	719	38	2.730	100	0.03	454	3	3.040	
BX313.....	2.323	0.15	905	32	2.880	∞	0.15	905	32	2.880	
BX341.....	2.117	0.05	905	25	2.280	∞	0.05	905	25	2.280	
BM1008	1.799	0.24	15	149	0.226	200	0.24	15	142	0.223	
BM1011	1.677	0.23	161	53	0.846	20	0.14	102	4	1.230	
BM1030	1.142	0.35	35	51	0.177	10	0.33	20	22	0.138	
BM1048	1.380	0.17	255	32	0.806	10	0.13	55	2	0.570	
BM1053	1.459	0.04	640	3	0.219	200	0.02	321	2	0.197	
BM1061	2.089	0.00	3000	4	1.070	∞	0.00	3000	4	1.070	
BM1063	2.087	0.10	3000	14	4.150	200	0.01	640	6	2.740	
BM1064	1.524	0.17	255	28	0.708	10	0.04	114	0	0.971	
BM1069	2.028	0.14	3000	29	8.650	500	0.06	1434	9	7.850	
BM1072	1.143	0.27	15	74	0.112	10	0.28	10	61	0.105	
BM1092	1.479	0.26	20	66	0.131	20	0.00	180	0	0.759	
BM1095	1.447	0.07	571	7	0.387	50	0.00	203	1	0.382	
BM1098	1.671	0.22	255	51	1.290	10	0.14	72	1	1.220	
BM1122	1.990	0.16	30	57	0.172	20	0.15	20	43	0.147	
BM1135	1.872	0.20	905	55	4.990	1000	0.20	640	52	4.660	
BM1139	1.919	0.07	1139	18	2.040	∞	0.07	1139	18	2.040	
BM1148	2.049	0.13	20	89	0.178	20	0.12	15	70	0.159	
BM1149	1.630	0.17	15	30	0.045	∞	0.17	15	30	0.045	
BM1153	2.444	0.12	2600	50	13.100	1000	0.04	2600	14	17.800	
BM1155	2.020	0.01	905	11	1.030	2000	0.00	806	10	1.040	
BM1159	1.016	0.12	286	19	0.533	100	0.10	180	11	0.568	
BM1160	1.364	0.23	128	20	0.255	10	0.10	90	0	0.440	
BM1161	2.045	0.00	2750	4	1.190	∞	0.00	2750	4	1.190	
BM1163	1.874	0.20	286	23	0.669	100	0.18	161	16	0.632	
BM1171	2.082	0.07	806	10	0.831	∞	0.07	806	10	0.831	
BM1172	1.864	0.08	321	13	0.423	1000	0.07	286	13	0.416	
BM1175	1.773	0.21	114	53	0.605	∞	0.21	114	53	0.605	
BM1180	1.598	0.18	806	32	2.580	100	0.10	321	10	2.320	
BM1181	1.743	0.30	7	645	0.467	∞	0.30	7	645	0.467	
BM1195	1.289	0.24	640	25	1.610	10	0.28	30	18	0.336	
BM1196	1.863	0.00	404	6	0.238	∞	0.00	404	6	0.238	
BM1197	1.566	0.20	360	30	1.090	10	0.09	114	0	1.280	
BM1198	1.780	0.30	15	203	0.307	10	0.31	10	169	0.290	
BM1200	2.078	0.09	640	23	1.490	1000	0.08	571	20	1.550	
BM1201	1.001	0.04	806	2	0.200	100	0.00	286	1	0.178	
BM1204	1.489	0.12	360	21	0.742	20	0.02	128	1	0.821	
BM1205	1.711	0.04	3500	8	2.720	1000	0.03	1434	7	2.090	
BM1207	1.083	0.31	15	57	0.087	50	0.35	10	88	0.098	

TABLE 3—*Continued*

Name[a]	z	$E(B-V)_\infty$	Age_∞ (Myr)	SFR_∞ ($M_\odot$ yr^{-1})	M^*_∞ (10^{10} $M_\odot$)	τ[b] (Myr)	$E(B-V)_\tau$	Age_τ (Myr)	SFR_τ ($M_\odot$ yr^{-1})	M^*_τ (10^{10} $M_\odot$)	Notes[c]
BM1209	1.775	0.34	10	365	0.365	10	0.32	9	222	0.331	
BM1226	1.355	0.35	10	104	0.104	50	0.34	10	90	0.099	
BM1289	2.380	0.23	8	139	0.115	10	0.23	7	108	0.114	
BM1299	1.595	0.35	114	203	2.320	5000	0.35	114	202	2.330	
BM1303	1.721	0.30	719	34	2.470	∞	0.30	719	34	2.470	
BM1334	1.893	0.24	509	58	2.930	100	0.17	255	25	2.900	
BM1335	1.489	0.51	10	1061	1.060	50	0.51	10	914	1.010	
BM1339	1.338	0.37	10	309	0.309	10	0.12	81	0	1.030	
BM1358	1.807	0.34	1278	81	10.400	500	0.32	719	63	10.100	
BM1369	1.879	0.41	7	277	0.200	50	0.44	6	394	0.253	
BM1375	2.109	0.07	2500	23	5.720	500	0.04	905	18	4.520	
BM1396	1.743	0.33	128	143	1.830	20	0.26	81	22	2.400	
BM72	1.571	0.19	1139	14	1.580	200	0.13	454	7	1.190	
C2	2.991	0.20	454	40	1.830	1000	0.34	40	163	0.666	
C11	2.990	0.31	9	326	0.297	20	0.01	114	2	0.895	
C12	2.975	0.39	10	891	0.891	10	0.12	81	1	2.520	
C14	2.973	0.46	8	779	0.648	50	0.46	8	694	0.628	
C16	2.929	0.46	9	2025	1.850	∞	0.46	9	2025	1.850	
C29	3.110	0.11	1015	26	2.690	100	0.00	360	6	2.160	
C30	3.328	0.04	454	25	1.140	200	0.00	321	15	1.160	
C33	3.130	0.03	454	36	1.650	5000	0.02	454	35	1.660	
C35	3.363	0.07	1680	28	4.660	500	0.04	806	20	3.970	
C41	3.148	0.04	2000	15	3.030	1000	0.00	2000	8	5.340	
C42	3.411	0.12	227	55	1.260	2000	0.12	227	53	1.260	
C48	3.206	0.26	15	179	0.270	50	0.02	180	6	1.050	
C53	3.103	0.30	9	249	0.227	200	0.30	9	243	0.227	
S03-C7	2.658	0.34	5	546	0.274	10	0.34	5	397	0.258	
S03-C8	2.988	0.12	255	45	1.140	50	0.00	203	5	1.460	
S03-C17	3.163	0.00	1900	11	2.140	5000	0.00	1900	11	2.470	
D14	2.979	0.04	2000	13	2.580	1000	0.04	1015	11	1.990	
D16	2.930	0.00	719	8	0.558	∞	0.00	719	8	0.558	
D23	3.125	0.06	1015	47	4.750	200	0.00	454	23	3.910	
D25	2.970	0.07	10	55	0.056	50	0.06	10	49	0.054	
D26	2.975	0.03	2100	7	1.500	2000	0.01	1800	6	1.630	
D28	2.932	0.41	9	1343	1.230	50	0.10	203	16	4.620	
D29	3.451	0.04	203	34	0.697	100	0.01	143	21	0.675	
D32	2.962	0.00	1015	9	0.944	∞	0.00	1015	9	0.944	
D34	2.972	0.14	1139	19	2.190	200	0.04	571	6	2.040	
D35	3.196	0.38	6	787	0.474	10	0.37	6	522	0.432	
D38	2.940	0.23	128	102	1.300	50	0.18	102	44	1.470	
D39	2.987	0.23	10	135	0.135	∞	0.23	10	135	0.135	
D47	3.191	0.00	1278	8	1.050	∞	0.00	1278	8	1.050	
D55	3.245	0.26	9	521	0.475	∞	0.26	9	521	0.475	
S03-oD3	2.725	0.00	806	11	0.906	500	0.00	509	10	0.882	
S03-oD12	2.418	0.28	25	129	0.324	10	0.27	15	74	0.262	
MD4	2.867	0.07	905	12	1.120	500	0.06	571	10	1.060	
MD6	3.243	0.05	1900	34	6.460	200	0.00	571	15	4.910	
MD13	2.974	0.19	321	112	3.600	50	0.04	227	9	4.190	
MD33	2.932	0.34	8	706	0.587	50	0.00	227	5	2.150	
MD48	2.926	0.16	1434	37	5.280	200	0.11	509	19	4.410	
MD49	2.850	0.29	9	485	0.442	50	0.00	203	6	1.780	
MD50	3.236	0.00	905	12	1.090	100	0.00	255	7	0.874	
MD54	2.939	0.12	1900	21	4.070	500	0.10	806	17	3.330	
MD55	2.956	0.20	128	60	0.761	50	0.08	161	10	1.160	
MD75	2.790	0.55	4	7037	2.800	50	0.55	4	6701	2.780	
MD83	3.213	0.00	404	18	0.717	∞	0.00	404	18	0.717	
S03-M16	2.939	0.01	2100	12	2.470	200	0.00	509	8	1.780	
S03-M25	3.106	0.00	1015	11	1.120	200	0.00	360	9	0.904	
S03-M35	3.229	0.35	10	910	0.910	10	0.34	9	558	0.830	

[a] We did not fit the stellar populations of galaxies that had no data longward of $\mathcal{R}$ band, had uncertain redshifts, or are identified as AGN/QSO from their optical spectra. We also do not present SED parameters for those galaxies with optical and IRAC photometry inconsistent with a simple stellar population (these sources had large $\chi^2 > 10$) or those sources with 8 or 24 μm excesses.

[b] Best-fit star formation history decay timescale. In some cases, a model with constant star formation ($\tau = \infty$) provided the best fit.

[c] Objects with large K_s band residuals are indicated (i.e., those sources whose K_s band measurement lies more than 3 σ away from the best-fit stellar population). MD31 is the only directly detected X-ray source that shows no optical signatures of an AGN, has a relatively faint 24 μm flux, and has photometry that is consistent with a stellar population. The IRAC photometry for BX1267 may suffer from a deblending problem, and these (IRAC) data were not used in the SED fit.

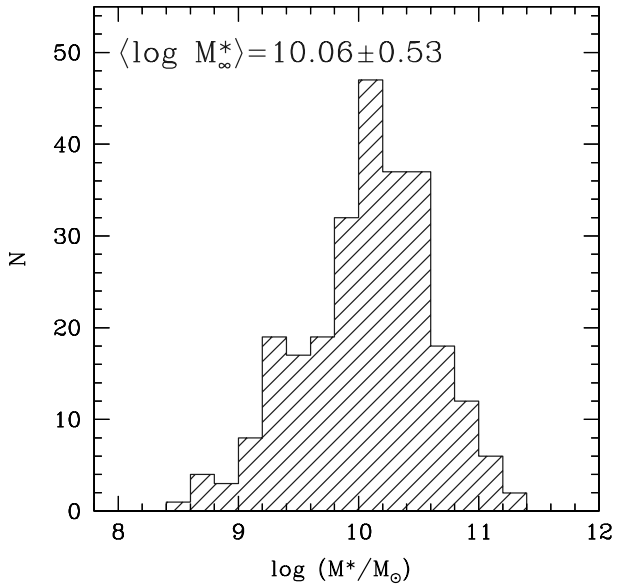

FIG. 4.—Stellar mass distribution of $U_nG\mathcal{R}$-selected galaxies with redshifts $z > 1$, assuming a CSF model. Assuming a best-fit exponentially declining star formation history (τ model) results in a stellar mass distribution that is virtually identical to the one shown here, with a mean and dispersion in log space of $\langle \log M^*_\tau \rangle = 10.08 \pm 0.51$. [*See the electronic edition of the Journal for a color version of this figure.*]

with the best-fit parameters (when including IRAC data in the fits) are $\langle \sigma_x/\langle x \rangle \rangle = 0.6$, 0.4, 0.5, and 0.2 in $E(B-V)$, age, SFR, and stellar mass, respectively (Erb et al. 2006c). For completeness we have included the best-fit SFRs from the fitting in Table 3, but we note that we have several other *independent* multiwavelength measures of the SFRs for these galaxies (e.g., from dust-corrected UV, Hα, and 24 μm data) that are unaffected by the degeneracies associated with stellar population modeling.

Aside from the systematic errors resulting from the degeneracy between star formation history and the best-fit parameters, there are additional caveats to the spectral energy distribution (SED) results. Around 30 objects had optical through IRAC photometry which is inconsistent with the stellar population models considered here; these objects exhibit large J/K_s *and* IRAC magnitude residuals with respect to the best-fit stellar population (and have $\chi^2 > 10$) and often give unrealistically young ages (<10 Myr) and large SFRs (>2000 $M_\odot$ yr^{-1}). We do not present the SED results for these galaxies. In addition to these 30, there are four galaxies that fit the optical and IRAC data well but have large K_s residuals with respect to the best-fit stellar population (i.e., a K_s magnitude more than 3 σ away from the best fit). Three of these four galaxies have redshifts $2.0 \le z \le 2.5$, where the K_s magnitude may be contaminated by emission from Hα+[N II]. The four galaxies with large K_s residuals are indicated by the notation "K_s" in Table 3. Also, we noted a few objects with 8 μm excesses when compared with the best-fit stellar population, many of which have large 24 μm fluxes ($f_{24\,\mu\mathrm{m}} > 100$ μJy), indicating that they may be obscured AGNs (see Table 5 below). We do not present SED fitting results for any of the sources that may have AGNs based on their 8 and 24 μm excesses and/or X-ray/optical emission. Finally, we did not perform SED fitting for galaxies without photometry longward of $\mathcal{R}$ band or that had redshifts $z < 1$. The best-fit SED parameters for the remaining 254 galaxies are listed in Table 3. Note that the SFRs and stellar masses (M^*) in Table 3 assume a Salpeter (1955) IMF from 0.1 to 100 $M_\odot$. Assuming the Chabrier (2003) IMF with a shallower faint-end slope results in SFRs and stellar masses a factor of 1.8 lower than listed in Table 3. We also note that a number of galaxies have inferred ages <50 Myr, which are unlikely given the dynamical timescale of ~50 Myr for star formation in galaxy-sized objects. The SED parameters for these galaxies with extremely young *inferred* ages should be taken with caution.

6. THE DIVERSE PROPERTIES OF OPTICALLY SELECTED GALAXIES AT HIGH REDSHIFT

6.1. *Star-forming Galaxies*

Of the best-fit SED parameters, the stellar mass is the least uncertain and is generally robust to changes in the assumed star formation history, as can be seen by comparing the sixth and eleventh columns in Table 3. Figure 4 shows the distribution of stellar masses for $U_nG\mathcal{R}$-selected galaxies with redshifts $z > 1$, assuming a constant star formation history. Table 4 shows the median and mean stellar masses and dispersion (assuming a CSF history) for galaxies in the various samples. While the mean stellar mass of the sample is $\langle M^* \rangle \approx 1.1 \times 10^{10}\ M_\odot$, there is large dispersion about this mean of a factor of 3.4. This mean stellar mass is a factor of ~2 lower than found in Shapley et al. (2005) and Erb et al. (2006c) partly because we included galaxies undetected to $K_s = 24.1$ in the sample considered here (as long as they had IRAC data to constrain the stellar mass), and these faint K_s galaxies on average have lower stellar masses than K_s-detected galaxies. Further, we have included BM galaxies, which have a mean stellar mass that is a factor of ≈2 lower than the mean stellar mass for BX galaxies and LBGs (Table 4). This difference in mean stellar mass likely reflects the fact that BM galaxies have a lower mean redshift ($z = 1.72 \pm 0.32$; Fig. 3) than BX galaxies and LBGs, and therefore we are able to probe down to fainter absolute magnitudes and are sensitive to lower mass galaxies.

Regardless, the sample includes galaxies with a wide range in ages, from young galaxies with ages comparable to the dynamical timescale for star formation of ~50 Myr to those that are older than 2 Gyr. In fact, the $U_nG\mathcal{R}$ sample includes galaxies that are as old (>2 Gyr) and as massive ($M^* > 10^{11}\ M_\odot$) as galaxies found at $z \sim 2$ in near-IR–selected samples (e.g., the distant red galaxies, or DRGs, of Franx et al. 2003).[10] In particular, Shapley et al. (2005) and Reddy et al. (2005) have shown that while the typical stellar mass of near-IR selected DRGs with $K_s \lesssim 21.8$ is larger by

[10] Optically selected galaxies that satisfy the DRG criteria ($J - K_s > 2.3$ in Vega magnitudes, or $J - K_s > 1.38$ in AB) are indicated by "DRG" in the last column of Table 2. There are 19 such DRGs with secure spectroscopic redshifts in our sample.

TABLE 4
STELLAR MASSES

Sample	N_{sed}[a]	$\log (M^*_{\mathrm{med}}/M_\odot)$[b]	$\log (M^*/M_\odot)$[c]
BM	51 (3)	9.87 (10.70)	9.85 ± 0.58 (10.58 ± 0.51)
BX.....	157 (7)	10.20 (10.98)	10.15 ± 0.52 (10.94 ± 0.38)
LBG.....	46 (0)	10.05 (...)	10.03 ± 0.44 (...)
Total	254 (10)	10.10 (10.98)	10.06 ± 0.53 (10.83 ± 0.43)

[a] Number of galaxies for which we derived best-fit SED parameters (including stellar mass), regardless of whether the galaxies were imaged at K_s. The parentheses indicate the number of galaxies with *measured* $K_s < 21.82$, or $K_s(\mathrm{Vega}) < 20$.

[b] Median stellar mass assuming a CSF history. Numbers in parentheses give the median stellar mass for those galaxies with $K_s < 21.82$, or $K_s(\mathrm{Vega}) < 20$.

[c] Mean and dispersion of stellar mass distribution assuming a CSF history. Numbers in parentheses give the mean stellar mass and dispersion for those galaxies with $K_s < 21.82$, or $K_s(\mathrm{Vega}) < 20$.

an order of magnitude than the *typical* stellar mass of $U_nG\mathcal{R}$-selected galaxies to $\mathcal{R} = 25.5$, the actual range in stellar mass probed by DRG selection does not appear to significantly exceed the range in stellar mass of $U_nG\mathcal{R}$-selected galaxies (although we note that DRG selection appears to be much more efficient in selecting galaxies with $M^* \gtrsim 10^{11}\ M_\odot$ at $z \sim 2$–3; e.g., van Dokkum et al. 2006). Further, SED analysis of the optically selected DRGs (as indicated in Table 2 by the notation "DRG" in the last column) with fainter near-IR magnitudes ($K_s \gtrsim 22.8$) shows that they have stellar masses that are comparable to the stellar masses of typical $U_nG\mathcal{R}$-selected galaxies ($10^9\ M_\odot \lesssim M^* \lesssim 10^{11}\ M_\odot$). While optical selection allows us to very efficiently follow up galaxies spanning over 2 orders of magnitude in age and stellar mass at redshifts $z \gtrsim 1.4$, other techniques are required to assess the total stellar mass budget at these redshifts (e.g., Rudnick et al. 2006; van Dokkum et al. 2006; Reddy et al. 2005).

While the $E(B - V)$ and SFRs determined from SED modeling are more uncertain than the inferred stellar masses, we have several independent methods of assessing the extinction and SFRs in $z \sim 2$ galaxies, made possible by the extensive multiwavelength data in the GOODS-N field. The exquisite, photon-limited *Chandra* X-ray data in the GOODS-N field, currently the deepest X-ray data ever taken (Alexander et al. 2003), allow for stacking analyses to estimate the average emission properties of galaxies (Brandt et al. 2001; Nandra et al. 2002; Reddy & Steidel 2004; Reddy et al. 2005). Based on the stacking analyses of Nandra et al. (2002) and Reddy & Steidel (2004), the mean SFR of $z \sim 2$–3 $U_nG\mathcal{R}$-selected galaxies is $\sim 50\ M_\odot\ \mathrm{yr}^{-1}$, with mean attenuation factors, defined as the ratio between the bolometric SFR and UV-based SFR (uncorrected for extinction), of 4.5–5.0.

The X-ray data allow us to determine the average extinction and SFRs of galaxies over the entire range of redshifts probed by the BX/BM and LBG criteria. However, important progress has been made in determining the individual properties of galaxies in a narrower redshift range, $1.5 \lesssim z \lesssim 2.6$, where the *Spitzer* MIPS 24 μm band is sensitive to the 7.7 μm polycyclic aromatic hydrocarbon (PAH) dust emission ubiquitous in local and high-redshift star-forming galaxies (Reddy et al. 2006; Papovich et al. 2006). Reddy et al. (2006) demonstrate that the 24 μm emission of $z \sim 2$ galaxies can be used as a tracer of the SFR or total infrared luminosity (L_{IR}), particularly for galaxies with spectroscopic redshifts where we are able to accurately constrain the K-corrections from 24 μm flux to rest-frame 5–8.5 μm luminosity. The MIPS data indicate that $U_nG\mathcal{R}$-selected galaxies at redshifts $1.5 \lesssim z \lesssim 2.6$ span more than 3 orders of magnitude in L_{IR}, from those that are undetected to the 3 σ sensitivity limit of 8 μJy for MIPS data in the GOODS field to those that have L_{IR} comparable to the most luminous star-forming galaxies at these redshifts, the submillimeter galaxies (Smail et al. 1997; Hughes et al. 1998; Barger et al. 1998; Chapman et al. 2005). The mean infrared luminosity for $U_nG\mathcal{R}$-selected galaxies is $\langle L_{\mathrm{IR}} \rangle \simeq 2 \times 10^{11}\ L_\odot$, assuming that the rest-frame infrared emission ($L_{5\text{–}8.5\ \mu\mathrm{m}}$) as probed by MIPS observations scales with infrared luminosity as $L_{\mathrm{IR}} \approx 17.2 L_{5\text{–}8.5\ \mu\mathrm{m}}$ as determined from local samples (see Reddy et al. 2006), and this value of $\langle L_{\mathrm{IR}} \rangle$ inferred from MIPS is in excellent agreement with X-ray and dust-corrected UV-based estimates. Reddy et al. (2006) further demonstrate that the agreement in SFR extends to galaxies on an individual (object-by-object) basis for a small sample of $U_nG\mathcal{R}$-selected galaxies with both 24 μm and Hα detections: the scatter between the bolometric luminosity inferred from 24 μm versus Hα observations is $\sim$0.2 dex. Finally, we have compared the 24 μm–estimated SFRs with those obtained from the SED fitting analysis: as expected, they are positively correlated at the 5 σ level with a scatter of 0.3 dex assuming a CSF model.[11] The advantage of multiwavelength data is that we can assess SFRs independent of the degeneracies associated with SED fitting. In summary, the $U_nG\mathcal{R}$-selected sample includes galaxies over 4 orders of magnitude in dust obscuration ($L_{\mathrm{bol}}/L_{\mathrm{UV}}$), from those galaxies with little dust and whose UV luminosity is comparable to L_{IR} to those that are heavily dust obscured and have attenuation factors $\gtrsim$1000.

Aside from the large dynamic range in SFRs and extinction of $U_nG\mathcal{R}$-selected galaxies, the sample also hosts galaxies with a wide range in morphology and kinematics (Erb et al. 2003, 2006c; Law et al. 2007), from disklike galaxies with signatures of rotation, as inferred from Hα spectral data (e.g., Forster Schreiber et al. 2006), to those galaxies that appear irregular and/or are merging. UV-selected samples efficiently target the redshift range where the morphological transformation of galaxies from irregular at high redshift to the Hubble sequence at low redshift ($z \lesssim 1.4$) takes place. The deep *HST* ACS data in the GOODS field (Giavalisco et al. 2004) combined with our extensive rest-frame UV spectroscopic database make it possible to study in detail the correlation between morphological structure and the SFRs, extinction, masses, and spectral properties of high-redshift galaxies (Law et al. 2007).

6.2. *AGNs*

The combination of X-ray, observed optical, 8 μm, and 24 μm data, along with spectroscopic redshifts, allows for a powerful probe of AGN activity among $U_nG\mathcal{R}$-selected galaxies. We classified objects as AGN based on one or more of the following criteria: (1) the presence of high-ionization UV lines (identical to the method used in Steidel et al. 2002; Shapley et al. 2005), (2) direct detection in the *Chandra* 2 Ms data (Alexander et al. 2003) and an X-ray–to–optical flux ratio indicative of AGNs (see, e.g., Hornschemeier et al. 2001; Reddy et al. 2005), or (3) an 8 and 24 μm flux excess above what one would expect from a simple star-forming population. Table 5 lists the 11 AGNs with confirmed redshifts $z > 1.4$ that have emission indicative of AGNs.

MD31 is the most unusual source: it has an X-ray counterpart within 1.″5 of the optical position but shows no evidence of AGNs from the rest-frame UV (observed optical) spectrum or from *Spitzer* observations. The SED analysis indicates that MD31 is best fitted with a $\sim$2 Gyr old population with a modest $E(B - V) \sim 0.17$ and SFR $\sim 60\ M_\odot\ \mathrm{yr}^{-1}$ assuming the CSF model and thus is not expected to be bright in X-rays as a result of star formation alone (i.e., the 2 Ms X-ray sensitivity implies a detection threshold of $\sim 480\ M_\odot\ \mathrm{yr}^{-1}$ at the redshift of MD31, $z = 2.981$). Examination of the deep ACS imaging in the GOODS field reveals no other optical counterpart within 1.″5 of MD31. If the X-ray counterpart is indeed associated with accretion activity in MD31, then the X-ray detection fraction of AGNs with $z > 1.4$ in our sample is 7/11, or 64%. On the other hand, the fraction of AGNs showing 8 and/or 24 μm excesses is 9/11, or 82%. While the object statistics are insufficient to judge the efficiency of AGN detection in the X-ray versus IR, we note that the IRAC and MIPS integration time for any given object in the GOODS-N field is $\sim$10 hr, whereas the X-ray integrations required to detect faint AGNs at redshifts $z \gtrsim 1.4$ are on the order of a megasecond or larger. The possible difference in AGN detection fraction and especially integration time between the IR and X-ray observations suggests that deep IR imaging may be a more efficient method of

[11] Adopting a declining model, as opposed to assuming a CSF model for all galaxies, will generally increase the scatter in SFRs since the youngest galaxies will have inferred SFRs (from declining star formation history models) that are systematically lower than those inferred from Hα observations (see discussion in Erb et al. 2006b).

TABLE 5
AGNs AT $z > 1.4$

Name	z	X-Ray?[a]	Optical?[b]	8 μm?[c]	24 μm?[d]	Notes[e]
BX1637	2.487	No	Yes (AGN)	Yes	Yes	ACS point source
BX160	2.460	No	Yes (AGN)	Yes	Yes	$K_s = 21.87$
BM1083	2.414	Yes	Yes (QSO)	Yes	Yes	
BM1119	1.717	Yes	No	Yes	Yes	$K_s = 21.74$
BM1156	2.211	No[f]	Yes (AGN)	Yes	Yes	Very weak X-ray source
BM1384	2.243	Yes	Yes (AGN)	Yes	No	$K_s = 21.69$
MD31	2.981	Yes	No	No	No	ACS point source
MD39	2.583	Yes	Yes (QSO)	Yes	Yes	$K_s = 20.07$
MD74	2.635	No	No	Yes	Yes	
S03-oC34	3.413	Yes	Yes (QS0)	No	No	
S03-MD12	2.647	Yes	Yes (AGN)	Yes	Yes	

[a] Indicates if the source lies within 1.″5 of an X-ray counterpart in the 2 Ms data (Alexander et al. 2003).
[b] Indicates if the source shows high-ionization optical emission lines indicative of AGNs/QSOs.
[c] Indicates if the source has a significant 8 μm excess compared with the flux at shorter wavelengths, larger than would be expected from a single stellar population.
[d] Indicates if the source has a 24 μm flux $f_{24\,\mu m} > 100$ μJy.
[e] K_s magnitudes are indicated for AGNs with $K_s < 21.82$, or K_s(Vega) $\lesssim 20$.
[f] BM1156 is not included in the *Chandra* 2 Ms catalogs, but further refinements to the X-ray data reduction procedure yielded a very weak detection (N. Brandt 2005, private communication).

finding AGNs at high redshifts. In this case, the 8 and 24 μm data indicate at least an additional three AGNs that are unidentified in X-rays. For comparison, while our optical spectra have integration times of 5400 s, a factor of 370 times shorter than the X-ray integration time (2 Ms), we can still detect ≈73% of AGNs based on their rest-frame UV emission lines.

The properties of the three X-ray–undetected AGNs with $z > 2$ are worth further consideration: these AGNs are BX1637, BX160, and MD74. Figure 5 shows the observed optical through 24 μm SEDs of these AGNs, as well as BM1156, which is very weakly detected in X-rays and demonstrates the power-law behavior at observed wavelengths longer than $\lambda \sim 2$ μm, indicative of the warm dust population. The three X-ray–undetected AGNs are also not detected in the deep radio imaging of the HDF (Richards 2000), placing a 3 σ upper limit on their observed 1.4 GHz flux of $f_{1.4\,\mathrm{GHz}} < 24$ μJy. However, all three have disturbed and/or extended rest-frame UV morphologies from deep ACS imaging (Giavalisco et al. 2004), suggesting that the obscured AGNs in these systems may be triggered by merger activity. The nondetection of these three AGNs (even when stacking them) in both the soft (0.5–2.0 keV) and full (2.0–8.0 keV) X-ray bands of *Chandra* makes it difficult to constrain their column densities. Nonetheless, these three AGNs have a mean spectroscopic redshift of $\langle z_{\mathrm{AGN}} \rangle \approx 2.5$, and if we assume that the AGNs have intrinsic photon index of $\Gamma = 2.0$ (e.g., Alexander et al. 2005), then we cannot rule out the possibility that these could be Compton-thick AGNs with column densities $N_{\mathrm{H}} > 10^{24}$ cm^{-2}. Comparison with the 8 and 24 μm fluxes of Mrk 463 and Mrk 1014, two infrared luminous AGNs (Armus et al. 2004), suggests that BX1637 and MD74 could have total infrared luminosities in the range 5×10^{12} $L_\odot \lesssim L_{\mathrm{IR}} \lesssim 2 \times 10^{13}$ $L_\odot$. Constraints on the 850 μm fluxes of these two AGNs could narrow the range of possible L_{IR}, but unfortunately submillimeter observations do not cover the region containing these two AGNs. BX160 is covered in published 850 μm imaging and is undetected to $S_{850} \sim 1.5$ mJy (Wang et al. 2004), suggesting an upper limit on the infrared luminosity of $\sim 10^{12.5}$ $L_\odot$. We caution, however, that the lack of data across the Raleigh-Jeans tail of the dust SEDs makes it difficult to accurately constrain the dust temperatures and hence total bolometric luminosities of these sources.

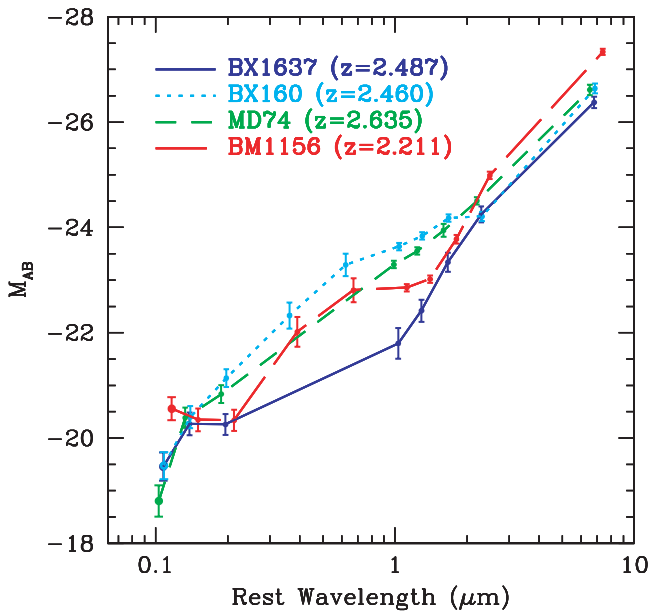

FIG. 5.—SEDs of the three X-ray–undetected AGNs (BX1637, BX160, and MD74) and one faint X-ray–detected AGN (BM1156) at $z = 2.211$–2.635 in the spectroscopic $U_nG\mathcal{R}$ sample, from observed optical through 24 μm. All four exhibit a power-law slope at long wavelengths ($\lambda \gtrsim 2$ μm rest frame) indicative of a warm dust population.

The presence of obscured AGNs at high redshifts has been postulated based on the expected fraction of high column density AGNs ($N_{\mathrm{H}} > 10^{23}$ cm^{-2}) at $z \gtrsim 1.4$ in simulations that model the contribution to the X-ray background (Comastri & Fiore 2004; Gilli 2004). While high column density AGNs may be unidentifiable as AGNs based on their optical spectra alone, the fact that some fraction of their host galaxies are optically bright ($\mathcal{R} < 25.5$) and fall within optically selected samples bodes well for determining their spectroscopic redshifts. Accurate spectroscopic redshifts are particularly important for constraining AGN column densities (N_{H}); the inferred N_{H} depends strongly on the assumed redshift, $N_{\mathrm{H}}(z) \approx N_{\mathrm{H}}(0)(1+z)^{2.6}$ (Alexander et al. 2005).

In summary, of the 11 AGNs with $z > 1.4$ in our optically selected sample, 7/11 (64%) are detected in X-rays to 2 Ms, 9/11

(82%) are detected with 8 and/or 24 μm excesses, and 8/11 (73%) have rest-frame UV signatures of AGNs. Even in the deepest X-ray image available, there is still a considerable number of AGNs that remain undetected, and we must incorporate other techniques, e.g., optical spectra and 8 and 24 μm data, to fully account for the census of AGNs.

7. SUMMARY

We have presented the results of a spectroscopic survey of redshift $1.4 \lesssim z \lesssim 3.0$ star-forming galaxies in the GOODS-North field, made possible by efficient UV ($U_nG\mathcal{R}$) color selection and the unique multiobject capabilities of the LRIS instrument on the Keck I telescope. Our sample consists of 212 redshifts for galaxies at redshifts $1.4 \lesssim z \lesssim 2.5$ selected using the BM and BX criteria of Adelberger et al. (2004) and Steidel et al. (2004) and 30 new redshifts (of a total of 74) for LBGs at redshifts $2.5 \lesssim z \lesssim 3.5$. Our deep optical and near-IR imaging, supplemented by publicly available *Spitzer* IRAC and MIPS data (M. Dickinson et al. 2006, in preparation; R. Chary et al. 2006, in preparation), allows us to measure the stellar populations, stellar masses, star formation rates, and dust extinction for galaxies in our sample (e.g., Erb et al. 2006c; Shapley et al. 2003, 2005; Reddy & Steidel 2004; Reddy et al. 2005, 2006; Steidel et al. 2004). These analyses indicate that the $U_nG\mathcal{R}$-selected sample consists of galaxies that span 2 orders of magnitude in age and stellar mass and 4 orders of magnitude in dust obscuration ($L_{\rm bol}/L_{\rm UV}$). Included are galaxies with bolometric star formation rates ranging from $\sim$5 to $>$1000 $M_\odot$ yr^{-1}. We further identify at least 3 of 11 AGNs in our sample that appear to be heavily dust obscured based on their power-law SEDs longward of 2 μm (rest frame) and lack of detection in the deep *Chandra* 2 Ms data (Alexander et al. 2003). A compilation of the multiwavelength data for these 11 AGNs indicates that optical and *Spitzer* data are able to more efficiently (in terms of integration time) select AGNs at $z > 1.4$ than X-ray data, but optical spectra and *Spitzer* and *Chandra* data are all required to fully account for the census of AGNs at high redshifts. The photometry and SED fitting results for galaxies in our sample are available online (see footnote 7).

Large spectroscopic samples at high redshifts allow for a number of other detailed investigations such as the galaxy and AGN/QSO luminosity functions (Steidel et al. 1999; Adelberger & Steidel 2000; Shapley et al. 2001; Hunt et al. 2004, N. A. Reddy et al. 2006, in preparation), metallicities (Pettini et al. 1998, 2001; Shapley et al. 2004; Erb et al. 2006a), signatures of galaxy feedback and IGM metal enrichment (Adelberger et al. 2003), and accurate clustering analyses (Adelberger et al. 2005a, 2005b). This large range in galaxy evolution studies highlights the versatility and efficiency of optically selected samples in addressing many fundamental issues in cosmology.

We thank David Law for setting up the Web site where the galaxy photometry and SED fits are available to the public. We are grateful to the staff of the Keck and Palomar Observatories for their help in obtaining the data presented here. This work has been supported by grant AST 03-07263 from the National Science Foundation and by the David and Lucile Packard Foundation.

REFERENCES

Adelberger, K. L., Erb, D. K., Steidel, C. C., Reddy, N. A., Pettini, M., & Shapley, A. E. 2005a, ApJ, 620, L75
Adelberger, K. L., Shapley, A. E., Steidel, C. C., Pettini, M., Erb, D. K., & Reddy, N. A. 2005b, ApJ, 629, 636
Adelberger, K. L., & Steidel, C. C. 2000, ApJ, 544, 218
Adelberger, K. L., Steidel, C. C., Shapley, A. E., Hunt, M. P., Erb, D. K., Reddy, N. A., & Pettini, M. 2004, ApJ, 607, 226
Adelberger, K. L., Steidel, C. C., Shapley, A. E., & Pettini, M. 2003, ApJ, 584, 45
Alexander, D. M., Bauer, F. E., Chapman, S. C., Smail, I., Blain, A. W., Brandt, W. N., & Ivison, R. J. 2005, ApJ, 632, 736
Alexander, D. M., et al. 2003, AJ, 126, 539
Armus, L., et al. 2004, ApJS, 154, 178
Barger, A. J., Cowie, L. L., & Richards, E. A. 2000, AJ, 119, 2092
Barger, A. J., Cowie, L. L., Sanders, D. B., Fulton, E., Taniguchi, Y., Sato, Y., Kawara, K., & Okuda, H. 1998, Nature, 394, 248
Barger, A. J., et al. 2003, AJ, 126, 632
Blain, A. W., Chapman, S. C., Smail, I., & Ivison, R. 2004, ApJ, 611, 725
Brandt, W. N., Hornschemeier, A. E., Schneider, D. P., Alexander, D. M., Bauer, F. E., Garmire, G. P., & Vignali, C. 2001, ApJ, 558, L5
Bruzual, G., & Charlot, S. 2003, MNRAS, 344, 1000
Capak, P., et al. 2004, AJ, 127, 180
Chabrier, G. 2003, PASP, 115, 763
Chapman, S. C., Blain, A. W., Ivison, R. J., & Smail, I. R. 2003, Nature, 422, 695
Chapman, S. C., Blain, A. W., Smail, I., & Ivison, R. J. 2005, ApJ, 622, 772
Cohen, J. G. 2001, AJ, 121, 2895
Cohen, J. G., Cowie, L. L., Hogg, D. W., Songaila, A., Blandford, R., Hu, E. M., & Shopbell, P. 1996, ApJ, 471, L5
Cohen, J. G., Hogg, D. W., Blandford, R., Cowie, L. L., Hu, E., Songaila, A., Shopbell, P., & Richberg, K. 2000, ApJ, 538, 29
Comastri, A., & Fiore, F. 2004, Ap&SS, 294, 63
Cowie, L. L., Barger, A. J., Hu, E. M., Capak, P., & Songaila, A. 2004, AJ, 127, 3137
Daddi, E., et al. 2004, ApJ, 600, L127
Dawson, S., Stern, D., Bunker, A. J., Spinrad, H., & Dey, A. 2001, AJ, 122, 598
Dickinson, M. 1998, in The Hubble Deep Field, ed. M. Livio, S. M. Fall, & P. Madau (New York: Cambridge Univ. Press), 219
Dickinson, M., Papovich, C., Ferguson, H. C., & Budavári, T. 2003a, ApJ, 587, 25
Dickinson, M., et al. 2003b, in The Mass of Galaxies at Low and High Redshift, ed. R. Bender & A. Renzini (Berlin: Springer), 324
Erb, D. K., Shapley, A. E., Pettini, M., Steidel, C. C., Reddy, N. A., & Adelberger, K. L. 2006a, ApJ, 644, 813
Erb, D. K., Shapley, A. E., Steidel, C. C., Pettini, M., Adelberger, K. L., Hunt, M. P., Moorwood, A. F. M., & Cuby, J.-G. 2003, ApJ, 591, 101
Erb, D. K., Steidel, C. C., Shapley, A. E., Pettini, M., Reddy, N. A., & Adelberger, K. L. 2006b, ApJ, 646, 107
———. 2006c, ApJ, 647, 128
Fan, X., et al. 2001, AJ, 121, 54
Forster Schreiber, N. M., et al. 2006, ApJ, 645, 1062
Franx, M., et al. 2003, ApJ, 587, L79
Giavalisco, M., et al. 2004, ApJ, 600, L93
Gilli, R. 2004, Adv. Space Res., 34, 2470
Hornschemeier, A. E., et al. 2001, ApJ, 554, 742
Hughes, D. H., et al. 1998, Nature, 394, 241
Hunt, M. P., Steidel, C. C., Adelberger, K. L., & Shapley, A. E. 2004, ApJ, 605, 625
Labbé, I., et al. 2005, ApJ, 624, L81
Law, D., et al. 2007, ApJ, in press
Lowenthal, J. D., et al. 1997, ApJ, 481, 673
Madau, P., Ferguson, H. C., Dickinson, M. E., Giavalisco, M., Steidel, C. C., & Fruchter, A. 1996, MNRAS, 283, 1388
Nandra, K., Mushotzky, R. F., Arnaud, K., Steidel, C. C., Adelberger, K. L., Gardner, J. P., Teplitz, H. I., & Windhorst, R. A. 2002, ApJ, 576, 625
Oke, J. B., & Gunn, J. E. 1983, ApJ, 266, 713
Oke, J. B., et al. 1995, PASP, 107, 375
Papovich, C., Dickinson, M., & Ferguson, H. C. 2001, ApJ, 559, 620
Papovich, C., et al. 2006, ApJ, 640, 92
Pettini, M., Kellogg, M., Steidel, C. C., Dickinson, M., Adelberger, K. L., & Giavalisco, M. 1998, ApJ, 508, 539
Pettini, M., Shapley, A. E., Steidel, C. C., Cuby, J.-G., Dickinson, M., Moorwood, A. F. M., Adelberger, K. L., & Giavalisco, M. 2001, ApJ, 554, 981
Phillips, A. C., Guzman, R., Gallego, J., Koo, D. C., Lowenthal, J. D., Vogt, N. P., Faber, S. M., & Illingworth, G. D. 1997, ApJ, 489, 543
Pope, A., Borys, C., Scott, D., Conselice, C., Dickinson, M., & Mobasher, B. 2005, MNRAS, 358, 149
Reddy, N. A., Erb, D. K., Steidel, C. C., Shapley, A., Adelberger, K. L., & Pettini, M. 2005, ApJ, 633, 748
Reddy, N. A., & Steidel, C. C. 2004, ApJ, 603, L13
Reddy, N. A., Steidel, C. C., Fadda, D., Yan, L., Pettini, M., Shapley, A. E., Erb, D. K., & Adelberger, K. L. 2006, ApJ, 644, 792

Richards, E. A. 2000, ApJ, 533, 611
Rudnick, G., et al. 2006, ApJ, 650, 624
Salpeter, E. E. 1955, ApJ, 121, 161
Sawicki, M., & Yee, H. K. C. 1998, AJ, 115, 1329
Schiminovich, D., et al. 2003, BAAS, 35, 1371
Schmidt, M., Schneider, D. P., & Gunn, J. E. 1995, AJ, 110, 68
Shapley, A. E., Erb, D. K., Pettini, M., Steidel, C. C., & Adelberger, K. L. 2004, ApJ, 612, 108
Shapley, A. E., Steidel, C. C., Adelberger, K. L., Dickinson, M., Giavalisco, M., & Pettini, M. 2001, ApJ, 562, 95
Shapley, A. E., Steidel, C. C., Erb, D. K., Reddy, N. A., Adelberger, K. L., Pettini, M., Barmby, P., & Huang, J. 2005, ApJ, 626, 698
Shapley, A. E., Steidel, C. C., Pettini, M., & Adelberger, K. L. 2003, ApJ, 588, 65
Shaver, P. A., Wall, J. V., Kellermann, K. I., Jackson, C. A., & Hawkins, M. R. S. 1996, Nature, 384, 439
Smail, I., Ivison, R. J., & Blain, A. W. 1997, ApJ, 490, L5
Steidel, C. C., Adelberger, K. L., Giavalisco, M., Dickinson, M., & Pettini, M. 1999, ApJ, 519, 1
Steidel, C. C., Adelberger, K. L., Shapley, A. E., Pettini, M., Dickinson, M., & Giavalisco, M. 2003, ApJ, 592, 728
Steidel, C. C., Giavalisco, M., Dickinson, M., & Adelberger, K. L. 1996, AJ, 112, 352
Steidel, C. C., & Hamilton, D. 1993, AJ, 105, 2017
Steidel, C. C., Hunt, M. P., Shapley, A. E., Adelberger, K. L., Pettini, M., Dickinson, M., & Giavalisco, M. 2002, ApJ, 576, 653
Steidel, C. C., Pettini, M., & Hamilton, D. 1995, AJ, 110, 2519
Steidel, C. C., Shapley, A. E., Pettini, M., Adelberger, K. L., Erb, D. K., Reddy, N. A., & Hunt, M. P. 2004, ApJ, 604, 534
van Dokkum, P. G., et al. 2006, ApJ, 638, L59
Vanzella, E., et al. 2005, A&A, 434, 53
Wang, W.-H., Cowie, L. L., & Barger, A. J. 2004, ApJ, 613, 655
Williams, R. E., et al. 1996, AJ, 112, 1335
———. 2000, AJ, 120, 2735
Wilson, J. C., et al. 2003, Proc. SPIE, 4841, 451
Wirth, G. D., et al. 2004, AJ, 127, 3121